Geophysical Journal International

Higher-order Hamilton-Jacobi perturbation theory for anisotropic heterogeneous media: Dynamic ray tracing in Cartesian coordinates

Journal:	*Geophysical Journal International*
Manuscript ID	Draft
Manuscript Type:	Research Paper
Date Submitted by the Author:	n/a
Complete List of Authors:	Iversen, Einar; Universitetet i Bergen Det Matematisk-naturvitenskapelige Fakultet, Department of Earth Science Ursin, Bjørn; NTNU, Geophysics Saksala, Teemu; Rice University, Computational and Applied Mathematics Ilmavirta, Joonas; Jyvaskylan Yliopisto, Department of Mathematics and Statistics de Hoop, Maarten; Rice University, Computational and Applied Mathematics
Keywords:	Numerical approximations and analysis < GEOPHYSICAL METHODS, Numerical modelling < GEOPHYSICAL METHODS, Body waves < SEISMOLOGY, Computational seismology < SEISMOLOGY, Seismic anisotropy < SEISMOLOGY, Wave propagation < SEISMOLOGY

Submitted manuscript

Higher-order Hamilton-Jacobi perturbation theory for anisotropic heterogeneous media: Dynamic ray tracing in Cartesian coordinates

Einar Iversen[1]

Bjørn Ursin[2]

Teemu Saksala[3]

Joonas Ilmavirta[4]

Maarten V. de Hoop[3]

[1] *University of Bergen, Department of Earth Science, P.O. Box 7803, N-5020 Bergen, Norway, e-mail: einar.iversen@uib.no*

[2] *Norwegian University of Science and Technology (NTNU), Department of Geoscience and Petroleum, S.P. Andersens vei 15A, NO-7491 Trondheim, Norway*

[3] *Rice University, Department of Computational and Applied Mathematics, 6100 Main MS-134, Houston, TX 77005-1892, USA*

[4] *University of Jyväskylä, Department of Mathematics and Statistics, P.O. Box 35 (MaD), FI-40014 University of Jyväskylä, Finland*

1 October 2018

SUMMARY

With a Hamilton-Jacobi equation in Cartesian coordinates as a starting point, it is common to use a system of ordinary differential equations describing the continuation of first-order phase-space perturbation derivatives along a reference ray. Such derivatives can be exploited for calculation of geometrical spreading on the reference ray, and for establishing a framework for second-order extrapolation of traveltime to points outside the reference ray. The continuation of the first-order phase-space perturbation derivatives has historically been referred to as dynamic ray tracing. The reason for this is its importance in the process of calculating amplitudes along the reference ray. We extend the standard dynamic ray tracing scheme to include higher orders in the phase-space perturbation derivatives. The main motivation is to extrapolate and interpolate important amplitude and phase properties of high-frequency Green's functions with better accuracy. Principal amplitude coefficients, geometrical spreading factors, traveltimes, slowness vectors, and curvature matrices are examples of quantities for which we enhance the computation potential. This, in turn, has immediate applications in modelling, mapping, and imaging. Numerical tests for 3D isotropic and anisotropic heterogeneous models yield clearly improved extrapolation results for traveltime and geometrical spreading. One important conclusion is that the extrapolation function for geometrical spreading must be at least third order to be appropriate at large distances away from the reference ray.

Key words: Numerical approximations and analysis; Numerical modelling; Body waves; Computational seismology, Seismic anisotropy; Wave propagation

1 INTRODUCTION

We consider higher-order Hamilton-Jacobi perturbation theory for anisotropic heterogeneous media. This theory arise from differentiation of the Hamilton system for ray tracing in phase space (Hamilton 1837). Specifically, we discuss the higher-order perturbations of a Hamiltonian flow with respect to its initial conditions in phase space.

The resulting perturbation coefficients can be used for higher-order extrapolation or interpolation of important quantities related to the amplitude and phase of the high-frequency Green's function: Traveltime, geometrical spreading, amplitude coefficients, polarization directions. The methodology has immediate applications in contexts where high-frequency Green's functions are used extensively, e.g., in modelling, mapping, and imaging.

The leading-order perturbation yields the linearized or first-order Hamilton-Jacobi perturbation system, the integration of which is commonly used, for example, to construct the geometrical spreading. In solid earth geophysics this process is known as dynamic ray tracing. We focus on integration of higher-order Hamilton-Jacobi perturbation equations — using point-source and local plane-wave initial conditions — in Cartesian phase-space coordinates.

Ray perturbation has been studied for decades commonly from a paraxial point of view (Červený 1972; Farra & Madariaga 1987; Bortfeld 1989; Hubral et al. 1992; Klimeš 1994; Červený 2001; Chapman 2004; Iversen 2004b; Moser & Červený 2007; Červený & Moser 2007; Iversen & Pšenčík 2008; Červený & Pšenčík 2010). We note that the leading-order perturbation of traveltime with respect to source and receiver location requires only the propagator associated with the linearized or first-order Hamilton-Jacobi system (Červený et al. 1984, 2012). Perturbation can be viewed as local extrapolation but can also be exploited for interpolation with derivatives. Our main motivation is *extrapolating* not only *traveltime* but also *geometrical spreading* away from a reference ray, that is, the geometrical spreading along a neighboring (paraxial) ray obtained by perturbation in phase space. We note that the integration of the higher-order Hamilton-Jacobi perturbation equations also opens for more accurate extrapolation of principal amplitude coefficients.

For higher-order derivatives of the traveltime only, in fact, one does not need to consider higher-order Hamilton-Jacobi perturbation equations (Goldin & Duchkov 2003). Indeed, for isotropic media Červený (2001) outlines a procedure by which higher-order derivatives of the traveltime can be obtained by a number of closed-form integrations along the reference ray. To our knowledge, however, this approach is not yet developed for anisotropic media; moreover, it will not be sufficient if the objective is also to permit non-trivial extrapolation of geometrical spreading.

The developed methodology has the following main applications:

- Fast computation of high-frequency elastic-wave Green's functions through (Hermite or spline) interpolation and extrapolation of amplitude and phase with derivatives. Our procedure holds in generally anisotropic media, leading to systems of equations describing the propagation of elastic waves, of principal type.
- Fast Generalized Radon Transform (GRT) inversion, where the amplitude and traveltime of the rays from the image point to the sources and receivers can be extrapolated from two reference rays (de Hoop et al. 1994; de Hoop & Bleistein 1997; Bleistein et al. 2001; Beylkin & Burridge 1990; Stolk & de Hoop 2002; Brandsberg-Dahl et al. 2003a,b; Sollid & Ursin 2003; Ursin 2004; Foss & Ursin 2004; Foss et al. 2004, 2005).
- Extrapolation from the reference rays of map depth migration (Iversen & Gjøystdal 1996; Douma & de Hoop 2006), with the assumption that the scattering is from interfaces. Asymptotically, one only needs a narrow fan of rays illuminating a reflector.
- True-amplitude time migration, that is, migration in image-ray coordinates and restricted-angle transform through extrapolation; here, the reference rays are image rays. This is considered a further development of earlier work on true-amplitude depth migration and time-to-depth mapping (Hubral 1977, 1983; Schleicher et al. 2007; Tygel et al. 2012; Iversen et al. 2012).

We make the observation that true-amplitude time migration formulated in this way explicitly shows that the relevant quantities can be obtained from the generalized Dix procedure for reconstruction of a Riemannian metric in ray-centred coordinates or Fermi coordinates (Cameron et al. 2007; Iversen & Tygel 2008; de Hoop et al. 2014, 2015).

- Ray-based extended depth imaging through extrapolation (Stolk & de Hoop 2006; de Hoop et al. 2009). Here, the reference rays are the ones for map migration.
- Map migration and depth imaging based on isochron rays (Iversen 2004a; Duchkov & de Hoop 2010).
- Source-receiver continuation and characterization of the range of the single scattering operator. Here, extrapolation provides the local flow along characteristic strips (de Hoop & Uhlmann 2006).
- Common-reflection-surface (CRS) processing techniques (e.g., Rabbel et al. 1991; Jäger et al. 2001). These techniques utilize that coherent local reflection events in the recorded data constitute a (hyper)surface, typically given in source-receiver coordinates or midpoint-offset coordinates (Ursin 1982). The CRS time surface is conventionally considered to be a second-

order approximation. When higher-order coefficients are available from ray theory one could consider an extension also of the CRS techniques to higher orders.

The paper is organized as follows. First, we describe the basic concepts of Hamilton-Jacobi theory, followed by a review of conventional dynamic ray tracing in Cartesian coordinates. Then, we introduce higher-order Hamilton-Jacobi phase-space perturbation equations and the constraint relations pertaining to them. We also specify initial conditions for the point-source and plane-wave situations. Assuming that the necessary phase-space perturbation data has been computed, we formulate approaches for higher-order paraxial extrapolation of traveltime and geometrical spreading. The Hamiltonian is mostly treated as a "black box" with certain fundamental properties. As we see it, this widens the number of applications where the theory can be used. One section is however devoted to specific Hamiltonians. After the theory sections we show numerical examples for three related 3D heterogeneous models. We also discuss briefly the connections to differential geometry. For an overview of the main mathematical symbols used in the paper, see Table 1.

2 HAMILTON-JACOBI EQUATION IN CARTESIAN PHASE SPACE

Consider a Cartesian coordinate system with the position vector $\mathbf{x} = (x_i)$ and slowness (momentum) vector $\mathbf{p} = (p_i)$. We form the phase space $\mathbf{w} = (w_r) = (x_i, p_j)$, where all six components vary freely. In the phase space (w_r) we further consider a reference ray Ω given as a function of the time τ, so that

$$w_r = \hat{w}_r(\tau). \tag{1}$$

Equation (1) can be associated with an equation of the Hamilton-Jacobi type,

$$\mathcal{H}(\mathbf{w}) = \hat{\mathcal{H}}\,, \tag{2}$$

where the function $\mathcal{H}(\mathbf{w})$ is referred to as the Hamiltonian, and $\hat{\mathcal{H}}$ is a nonzero constant. The Hamilton-Jacobi equation (2) is a nonlinear first-order partial differential equation for the time τ along Ω— in the context of wave propagation it is also often called the Eikonal equation.

One can interpret equation (2) to represent a hypersurface (manifold) in phase space with five degrees of freedom. This hypersurface is typically not available as a specific, exact, function; rather, it will be known through derivatives evaluated up to a certain order with respect to phase-space coordinates at points on Ω.

We assume that $\mathcal{H}$ is a homogeneous function of degree two in the slowness components,

p_i. Then, Euler's theorem for homogeneous functions yields

$$p_i \frac{\partial \mathcal{H}}{\partial p_i} = 2\,\mathcal{H}\,. \tag{3}$$

The specific formulation chosen for the Hamiltonian will determine what will be the independent variable along rays. For this variable to be the time τ, the Hamiltonian must satisfy

$$p_i \frac{\partial \mathcal{H}}{\partial p_i} \;=\; 1. \tag{4}$$

In view of equation (3) the constant in equation (2) is therefore $\hat{\mathcal{H}} = 1/2$.

The total temporal derivatives of position and momentum vectors can be computed using Hamilton's equations,

$$\frac{\mathrm{d}x_i}{\mathrm{d}\tau} = \frac{\partial \mathcal{H}}{\partial p_i}, \qquad \frac{\mathrm{d}p_i}{\mathrm{d}\tau} = -\frac{\partial \mathcal{H}}{\partial x_i}. \tag{5}$$

Integration of the ordinary differential equations (ODEs) in equation (5) yields the solution functions $\hat{x}_i(\tau)$ and $\hat{p}_i(\tau)$ on Ω, as well as the time derivative of these functions,

$$v_i(\tau) = \frac{\mathrm{d}\hat{x}_i}{\mathrm{d}\tau}(\tau), \qquad \eta_i(\tau) = \frac{\mathrm{d}\hat{p}_i}{\mathrm{d}\tau}(\tau). \tag{6}$$

We note that $\mathbf{v} = (v_i)$ signifies the ray-velocity (group-velocity) vector, while the time derivative of the slowness vector, $\boldsymbol{\eta} = (\eta_i)$, is referred to as just the eta vector. The fundamental requirement in equation (4) and the first sub-equations of (5)–(6) show that the slowness vector and ray-velocity vector must satisfy

$$p_i v_i = 1 \tag{7}$$

along the ray Ω.

Hamilton's equations may alternatively be formulated compactly as

$$\frac{\mathrm{d}w_r}{\mathrm{d}\tau} = J_{rs} \frac{\partial \mathcal{H}}{\partial w_s}, \tag{8}$$

where J_{rs} are components of the 6×6 matrix

$$\mathbf{J} = \{J_{rs}\} = \begin{pmatrix} \{0_{ij}\} & \{\delta_{ij}\} \\ -\{\delta_{ij}\} & \{0_{ij}\} \end{pmatrix}. \tag{9}$$

The right-hand side of equation (8) is the Hamiltonian vector field corresponding to the Hamiltonian $\mathcal{H}$.

Differentiation of equation (3) with respect to p_i yields the important relation

$$\frac{\partial^2 \mathcal{H}}{\partial p_i \partial p_j}\, p_j = \frac{\partial \mathcal{H}}{\partial p_i}, \tag{10}$$

which holds for general locations in phase space. For other useful expressions involving derivatives of the Hamiltonian, see Appendix A.

On the ray Ω equation (10) is recast to

$$V_{ij}(\tau)\ \hat{p}_j(\tau)\ =\ v_i(\tau), \tag{11}$$

where

$$V_{ij}(\tau)\ =\ \frac{\partial^2 \mathcal{H}}{\partial p_i \partial p_j}(\hat{\mathbf{w}}(\tau)). \tag{12}$$

In physics, the quantity $\{V_{ij}\}$ is often referred to as the wave-propagation metric tensor (Klimeš 2002a). In Riemannian geometry (e.g., Bao et al., 2012), the hypersurface (2) is approximated using partial derivatives of slowness components up to order two taken on the ray Ω. As a consequence, the second-order derivatives $\partial^2 \mathcal{H}/\partial p_i \partial p_j$ are considered invariant with respect to $\mathbf{p}$.

3 CONVENTIONAL DYNAMIC RAY TRACING

As an introduction to higher-order Hamilton-Jacobi perturbation equations, we summarize the basics of conventional dynamic ray tracing.

3.1 Perturbations in phase space

Consider again a reference ray Ω with phase-space locations $(\hat{w}_r(\tau))$ consistent with equation (2). A perturbed phase-space location is then generally expressed as

$$w_r\ =\ \hat{w}_r(\tau) + \delta w_r, \tag{13}$$

where all six perturbation components δw_r may vary freely. It is common to write the perturbed phase-space location as a vectorial function, with components $w_r = w_r(\boldsymbol{\gamma}, \tau)$. Here, the vector $\boldsymbol{\gamma} = (\gamma_a)$ has dimension N_γ and serves to parametrize a perturbation of the phase-space location corresponding to the initial point on Ω, for which $\tau = \tau_0$. The symbol $\hat{\boldsymbol{\gamma}}$ signifies no perturbation of this initial phase-space location. We require i) that the variables γ_a are mutually independent, ii) that none of them depend on the time, τ, and iii) that none of them depend on the model of the medium. It follows that the dimension, N_γ, of the vector $\boldsymbol{\gamma}$ must have the maximum value $N_\gamma = 6$, i.e., the dimension of the Cartesian phase space.

3.2 System of Hamilton-Jacobi perturbation equations

A system for *dynamic ray tracing* in Cartesian coordinates (x_i) can be derived by inserting equation (13) on the left-hand side of equation (8) followed by partial differentiation with respect to the variable γ_a. Since τ and γ_a are independent variables, the differentiations $\mathrm{d}/\mathrm{d}\tau$

and $\partial/\partial\gamma_a$ commute (Červený, 2001; section 4.2.1). We obtain the system of ODEs

$$\frac{\mathrm{d}X_{ra}}{\mathrm{d}\tau}(\tau) = S_{rt}(\tau)\, X_{ta}(\tau); \qquad \frac{\mathrm{d}\mathbf{X}}{\mathrm{d}\tau}(\tau) = \mathbf{S}(\tau)\, \mathbf{X}(\tau), \tag{14}$$

where $X_{ra}(\tau)$ can be equivalently defined by by the partial derivatives

$$X_{ra}(\tau) \;=\; \frac{\partial(\delta w_r)}{\partial\gamma_a}(\hat{\boldsymbol{\gamma}},\tau) \;=\; \frac{\partial w_r}{\partial\gamma_a}(\hat{\boldsymbol{\gamma}},\tau), \tag{15}$$

and $S_{rt}(\tau)$ is formed by the second partial derivatives of the Hamiltonian,

$$S_{rt}(\tau) = J_{rs}\, \frac{\partial^2 \mathcal{H}}{\partial w_s \partial w_t}[\mathbf{w}(\hat{\boldsymbol{\gamma}},\tau)]. \tag{16}$$

The quantity X_{ra} in equation (15) is a first-order phase-space *perturbation derivative* related to a point with time τ on the reference ray Ω. For clarity of notation, we prefer mostly to write such derivatives as in the last expression of equation (15), i.e., without the perturbation (δ) symbol. It is emphasized that the derivative $\partial w_r/\partial\gamma_a$ belongs to a fixed value of the time τ.

Conventional dynamic ray tracing in Cartesian coordinates yields as output the $6 \times N_\gamma$ matrix $\mathbf{X}(\tau) = \{X_{ra}(\tau)\}$, with components of the form given in equation (15). The matrix function $\mathbf{X}(\tau)$ is continued along the ray Ω by solving the system of ODEs in equation (14) with suitable initial conditions. It is common to split the matrix $\{X_{ra}\}$ into $3\times N_\gamma$ sub-matrices $\{Q_{ma}\}$ and $\{P_{ma}\}$, such that

$$Q_{ma}(\tau) = \frac{\partial x_m}{\partial\gamma_a}(\hat{\boldsymbol{\gamma}},\tau), \qquad P_{ma}(\tau) = \frac{\partial p_m}{\partial\gamma_a}(\hat{\boldsymbol{\gamma}},\tau). \tag{17}$$

Equation (14) can therefore be written equivalently as

$$\frac{\mathrm{d}}{\mathrm{d}\tau}\begin{pmatrix} \mathbf{Q}(\tau) \\ \mathbf{P}(\tau) \end{pmatrix} \;=\; \begin{pmatrix} \mathbf{W}^T(\tau) & \mathbf{V}(\tau) \\ -\mathbf{U}(\tau) & -\mathbf{W}(\tau) \end{pmatrix} \begin{pmatrix} \mathbf{Q}(\tau) \\ \mathbf{P}(\tau) \end{pmatrix}, \tag{18}$$

with

$$U_{ij}(\tau) = \frac{\partial^2 \mathcal{H}}{\partial x_i \partial x_j}[\mathbf{w}(\hat{\boldsymbol{\gamma}},\tau)], \quad V_{ij}(\tau) = \frac{\partial^2 \mathcal{H}}{\partial p_i \partial p_j}[\mathbf{w}(\hat{\boldsymbol{\gamma}},\tau)] \;, \quad W_{ij}(\tau) = \frac{\partial^2 \mathcal{H}}{\partial x_i \partial p_j}[\mathbf{w}(\hat{\boldsymbol{\gamma}},\tau)]. \tag{19}$$

Here, V_{ij} represents the wave-propagation metric tensor components introduced in equation (12). Dynamic ray tracing, prescribed by the Hamilton-Jacobi perturbation equations (18), may be performed simultaneously or subsequently with respect to ray tracing, prescribed by Hamilton's equations (5). In the latter case, the functions $\hat{\mathbf{x}}(\tau)$ and $\hat{\mathbf{p}}(\tau)$ will be known beforehand; the same is true for the functions $\mathbf{v}(\tau)$ and $\boldsymbol{\eta}(\tau)$ in equation (6).

3.3 Ray propagator matrix

There are two common ways to find a solution of the system of ODEs in equation (14) or (18) by means of integration. One is to integrate with right-hand sides of the differential equations

exactly as specified in (14) or (18), the other is to make use of a precalculated (known) first-order mapping between perturbed phase-space locations at the start and end point of the ray Ω. The coefficients of this mapping form the 6×6 ray propagator matrix in Cartesian coordinates. Below we introduce this matrix in a formal way.

A situation of particular interest arises if we choose the vector $\boldsymbol{\gamma}$ specifically as the six-dimensional phase-space perturbation at the initial point on Ω, for which $\tau = \tau_0$, that means,

$$\gamma_r = (\delta w_r)_0 = w_r - \hat{w}_r(\tau_0). \tag{20}$$

Obviously, for this definition of $\boldsymbol{\gamma}$ we have $\hat{\boldsymbol{\gamma}} = \mathbf{0}$, the six-component zero vector. Using equation (13), we establish the function

$$\delta w_r(\delta \mathbf{w}_0, \tau) = w_r(\delta \mathbf{w}_0, \tau) - \hat{w}_r(\tau), \tag{21}$$

where it is implicit that the freely varying (perturbation) vector $\delta \mathbf{w}_0$ belongs to the time τ_0. The ray propagator matrix of size 6×6 in Cartesian coordinates can then be introduced as

$$\Pi_{ru}(\tau, \tau_0) \quad = \quad \frac{\partial(\delta w_r)}{\partial(\delta w_u)_0} \; (\delta \mathbf{w}_0 = \mathbf{0}, \tau). \tag{22}$$

The ray propagator matrix encapsulates the six fundamental solutions to the system (14) of ODEs. The Hamilton-Jacobi perturbation equations for the ray propagator matrix are given by

$$\frac{\mathrm{d}\Pi_{ru}}{\mathrm{d}\tau}(\tau, \tau_0) = S_{rt}(\tau)\, \Pi_{tu}(\tau, \tau_0); \qquad \frac{\mathrm{d}\boldsymbol{\Pi}}{\mathrm{d}\tau}(\tau, \tau_0) = \mathbf{S}(\tau)\, \boldsymbol{\Pi}(\tau, \tau_0), \tag{23}$$

with the initial condition

$$\Pi_{ru}(\tau_0, \tau_0) = \delta_{ru}. \tag{24}$$

When the ray propagator matrix is known for the segment (τ, τ_0) of the ray Ω, any other dynamic ray-tracing solution on that segment can be computed using the linear combination of fundamental solutions,

$$X_{ra}(\tau) = \Pi_{rt}(\tau, \tau_0) X_{ta}(\tau_0); \qquad \mathbf{X}(\tau) = \boldsymbol{\Pi}(\tau, \tau_0) \mathbf{X}(\tau_0). \tag{25}$$

In this way, the ray propagator matrix $\boldsymbol{\Pi}(\tau, \tau_0)$ represents the solution operator for the initial value problem (14).

The initial perturbation $\boldsymbol{\gamma} = \delta \mathbf{w}_0$ encompasses six degrees of freedom. A general perturbation $\delta \mathbf{w}_0$ can be considered to consist of i) a *paraxial* contribution (four degrees of freedom), ii) a *ray-tangent* contribution (one degree of freedom), and iii) a *non-eikonal* contribution (one degree of freedom). The particular fundamental solutions resulting from these three types of initial conditions are often referred to as the paraxial, ray-tangent, and non-eikonal solutions of dynamic ray tracing (Červený 2001).

3.4 Dynamic ray tracing specified by two paraxial ray parameters

Consider a situation with two parameters specifying the initial phase-space perturbation ($N_\gamma = 2$). For this particular situation we replace lowercase indices a and b in equation (17) with corresponding uppercase indices A and B. We further assume that the parameters γ_A, $A = 1, 2$, have a purely paraxial nature, so that any initial phase-space perturbation is constrained not to have a ray-tangent or non-eikonal contribution. The parameters γ_A specify the initial conditions for paraxial rays, that means, rays in the vicinity of the reference ray Ω. We refer to γ_A as paraxial ray parameters or just *ray parameters*. For any reference ray or paraxial ray, the ray parameters are constant.

Together, the two quantities γ_A and the traveltime τ form a three-dimensional curvilinear *ray coordinate system*, $(\gamma_1, \gamma_2, \tau)$. The mapping from ray coordinates to Cartesian coordinates reads

$$x_i = x_i(\gamma_1, \gamma_2, \tau), \qquad p_i = p_i(\gamma_1, \gamma_2, \tau). \tag{26}$$

We introduce 3×3 matrices $\widehat{\mathbf{Q}}$ and $\widehat{\mathbf{P}}$ for performing first-order transformation of position and momentum vectors from ray coordinates to Cartesian coordinates. The components of these matrices are

$$Q_{iA} = \frac{\partial x_i}{\partial \gamma_A}, \qquad Q_{i3} = \frac{\partial x_i}{\partial \tau}, \tag{27}$$

$$P_{iA} = \frac{\partial p_i}{\partial \gamma_A}, \qquad P_{i3} = \frac{\partial p_i}{\partial \tau}. \tag{28}$$

Matrix $\widehat{\mathbf{Q}}$ is the 3×3 geometrical spreading matrix for dynamic ray tracing in Cartesian coordinates.

For the inverse mapping operation, from Cartesian coordinates to ray coordinates, we introduce the *ray parameter function* $\gamma_A(\mathbf{x})$ and the *traveltime function* $\tau(\mathbf{x})$,

$$\gamma_A = \gamma_A(\mathbf{x}), \qquad \tau = \tau(\mathbf{x}), \tag{29}$$

with first-order derivatives

$$\frac{\partial \gamma_A}{\partial x_i} = Q^\dagger_{Ai}, \qquad \frac{\partial \tau}{\partial x_i} = p_i = Q^\dagger_{3i}. \tag{30}$$

The quantities $Q^\dagger_{ai}$ in equation (30) form the inverse of matrix $\widehat{\mathbf{Q}}$, such that

$$\widehat{\mathbf{Q}}^{-1} = \widehat{\mathbf{Q}}^\dagger. \tag{31}$$

More details on the first-order transformation between ray coordinates and Cartesian coordinates are given in Appendix B.

For the second derivatives of the traveltime function $\tau(\mathbf{x})$ we use the notation

$$\mathbf{M} \;=\; \{M_{ij}\} \;=\; \left\{ \frac{\partial^2 \tau}{\partial x_i \partial x_j} \right\}. \tag{32}$$

It is straightforward to show (see Appendix B) that matrix $\mathbf{M}$ can be computed using

$$\mathbf{M} = \widehat{\mathbf{P}}\widehat{\mathbf{Q}}^{-1}. \tag{33}$$

4 HIGHER-ORDER HAMILTONIAN-JACOBI PERTURBATION EQUATIONS

In conventional dynamic ray tracing in Cartesian coordinates one continues along the ray Ω the first-order derivatives of a phase-space perturbation, given in equation (15). That approach is extended here to include continuation of derivatives up to third order.

4.1 Continuation of second-order phase-space perturbation derivatives

We formulate second-order phase-space perturbation derivatives compactly as

$$X_{rab}(\tau) = \frac{\partial^2 w_r}{\partial \gamma_a \partial \gamma_b}(\hat{\boldsymbol{\gamma}}, \tau). \tag{34}$$

In Q-P notation we write them as

$$Q_{iab}(\tau) = \frac{\partial^2 x_i}{\partial \gamma_a \partial \gamma_b}(\hat{\boldsymbol{\gamma}}, \tau), \qquad P_{iab}(\tau) = \frac{\partial^2 p_i}{\partial \gamma_a \partial \gamma_b}(\hat{\boldsymbol{\gamma}}, \tau). \tag{35}$$

We map the third-order derivatives of the Hamiltonian to a three-dimensional coefficient tensor,

$$S_{rtu}(\tau) = J_{rs} \, \frac{\partial^3 \mathcal{H}}{\partial w_s \partial w_t \partial w_u}[w_z(\hat{\boldsymbol{\gamma}}, \tau)]. \tag{36}$$

Using the latter, we establish ODEs for continuation of second-order phase-space perturbation derivatives,

$$\frac{\mathrm{d}X_{rab}}{\mathrm{d}\tau}(\tau) = S_{rt}(\tau) X_{tab}(\tau) + R_{rab}(\tau), \tag{37}$$

where

$$R_{rab}(\tau) = S_{rtu}(\tau) X_{ta}(\tau) X_{ub}(\tau). \tag{38}$$

The combination of ODEs given by equations (14) and (37) can be integrated to yield the solution (34).

A different approach is to use an expression for the solution in terms of the initial condition, the ray propagator matrix, and a closed-form integral along the ray Ω,

$$X_{rab}(\tau) = \Pi_{rt}(\tau, \tau_0) X_{tab}(\tau_0) + \int_{\tau_0}^{\tau} \Pi_{rt}(\tau, \tau') \, R_{tab}(\tau') \, \mathrm{d}\tau'. \tag{39}$$

This approach requires that the ray propagator matrix, $\Pi_{rt}(\tau, \tau_0)$, is a known (precomputed) function.

It is convenient to reformulate equation (39) such that the ray propagator matrix in the integrand corresponds to propagation from $\tau = \tau_0$ to $\tau = \tau'$. Using the chain property and the symplectic property of the ray propagator matrix we obtain

$$X_{rab}(\tau) = \Pi_{rt}(\tau, \tau_0) \left(X_{tab}(\tau_0) - \int_{\tau_0}^{\tau} J_{tv} \Pi_{sv}(\tau', \tau_0) J_{sq} \, R_{qab}(\tau') \, \mathrm{d}\tau' \right). \tag{40}$$

4.2 Continuation of third-order phase-space perturbation derivatives

We want to determine phase-space perturbation derivatives of third order,

$$X_{rabc}(\tau) = \frac{\partial^3 w_r}{\partial \gamma_a \partial \gamma_b \partial \gamma_c}(\hat{\boldsymbol{\gamma}}, \tau), \tag{41}$$

or in Q-P notation,

$$Q_{iabc}(\tau) = \frac{\partial^3 x_i}{\partial \gamma_a \partial \gamma_b \partial \gamma_c}(\hat{\boldsymbol{\gamma}}, \tau), \qquad P_{iabc}(\tau) = \frac{\partial^3 p_i}{\partial \gamma_a \partial \gamma_b \partial \gamma_c}(\hat{\boldsymbol{\gamma}}, \tau). \tag{42}$$

The ODEs for continuation of third-order phase-space perturbation derivatives can be written,

$$\frac{\mathrm{d}X_{rabc}}{\mathrm{d}\tau}(\tau) = S_{rt}(\tau) X_{tabc}(\tau) + R_{rabc}(\tau), \tag{43}$$

where

$$S_{rtuv}(\tau) = J_{rs} \, \frac{\partial^4 \mathcal{H}}{\partial w_s \partial w_t \partial w_u \partial w_v}[w_z(\hat{\boldsymbol{\gamma}}, \tau)], \tag{44}$$

$$\begin{aligned} R_{rabc}(\tau) \;\; = \;\; & S_{rtu}(\tau) \left[X_{ta}(\tau) X_{ubc}(\tau) \, + \, X_{tb}(\tau) X_{uac}(\tau) \, + \, X_{uc}(\tau) X_{tab}(\tau) \right] \\ & + \, S_{rtuv}(\tau) \, X_{ta}(\tau) \, X_{ub}(\tau) \, X_{vc}(\tau). \end{aligned} \tag{45}$$

The ODEs given by equations (14), (37), and (43) can be integrated to yield the solution (41).

Alternatively we write the solution in terms of its initial condition, the ray propagator matrix, and a closed-form integral along the ray Ω,

$$X_{rabc}(\tau) = \Pi_{rt}(\tau, \tau_0) X_{tabc}(\tau_0) + \int_{\tau_0}^{\tau} \Pi_{rt}(\tau, \tau') R_{tabc}(\tau') \mathrm{d}\tau'. \tag{46}$$

In this situation $\Pi_{rt}(\tau, \tau_0)$ and $X_{tab}(\tau)$ must be known along Ω. The chain and symplectic properties of the ray propagator matrix yield

$$X_{rabc}(\tau) = \Pi_{rt}(\tau, \tau_0) \left(X_{tabc}(\tau_0) - \int_{\tau_0}^{\tau} J_{tv} \Pi_{sv}(\tau', \tau_0) J_{sq} \, R_{qabc}(\tau') \, \mathrm{d}\tau' \right). \tag{47}$$

Equation (47) represents a third-order analogue of equation (40).

5 CONSTRAINT RELATIONS

Perturbation derivatives in phase space are in general not independent, as they will be constrained by the Hamiltion-Jacobi equation (2). To describe dependencies between first-order perturbation derivatives in conventional dynamic ray tracing Červený (2001) uses the notion *constraint relation*. When introducing perturbation derivatives of higher order it is necessary to consider also higher-order constraint relations.

5.1 Constraint relation for first-order phase-space perturbation derivatives

The Hamiltonian is required to be constant along a trajectory in the phase space. As a consequence,

$$\frac{\partial \mathcal{H}}{\partial w_r}\frac{\partial w_r}{\partial \gamma_a} = 0, \quad \text{or equivalently,} \quad \frac{\partial \mathcal{H}}{\partial x_i}\frac{\partial x_i}{\partial \gamma_a} + \frac{\partial \mathcal{H}}{\partial p_i}\frac{\partial p_i}{\partial \gamma_a} = 0. \tag{48}$$

Thus, along Ω the following constraint applies,

$$v_i P_{ia} = \eta_i Q_{ia}. \tag{49}$$

Equation (49) represents the constraint relation for first-order phase-space perturbation derivatives in Cartesian coordinates (Červený 2001).

5.2 Constraint relations for second-order phase-space perturbation derivatives

Differentiation of equation (48) with respect to γ_b yields

$$\frac{\partial^2 \mathcal{H}}{\partial w_r \partial w_s}\frac{\partial w_r}{\partial \gamma_a}\frac{\partial w_s}{\partial \gamma_b} + \frac{\partial \mathcal{H}}{\partial w_r}\frac{\partial^2 w_r}{\partial \gamma_a \partial \gamma_b} = 0. \tag{50}$$

We use

$$\begin{aligned} \frac{\partial \mathcal{H}}{\partial w_r} &= -J_{rs}\dot{w}_s, \\ \frac{\partial^2 \mathcal{H}}{\partial w_r \partial w_s} &= -J_{rt}S_{ts}, \end{aligned}$$

so that equation (50) becomes

$$-J_{rt}S_{ts}X_{ra}X_{sb} - J_{rs}\dot{w}_s X_{rab} = 0. \tag{51}$$

Applying the standard Hamilton-Jacobi perturbation equations (14) then yields the second-order constraint relation,

$$-X_{rab}J_{rs}\dot{w}_s = X_{ra}J_{rs}\dot{X}_{sb}. \tag{52}$$

In Q-P notation the latter equation is restated

$$v_i P_{iab} = \eta_i Q_{iab} + Q_{ia}\dot{P}_{ib} - P_{ia}\dot{Q}_{ib}. \tag{53}$$

For a situation with two paraxial ray parameters γ_A, $A = 1, 2$, we may introduce in equation (53) the 3×3 matrix $\mathbf{M}$ of second derivatives of traveltime, defined in equation (33), so that

$$v_i P_{iAB} = \eta_i Q_{iAB} + \dot{M}_{ij} Q_{iA} Q_{jB}. \tag{54}$$

5.3 Constraint relations for third-order phase-space perturbation derivatives

We differentiate equation (52) with respect to γ_c. Since the quantities γ_c are independent of the traveltime τ, the order of differentiation in γ_c and τ can be interchanged. We then obtain the third-order constraint relation,

$$-X_{rabc} J_{rs} \dot{w}_s = X_{rab} J_{rs} \dot{X}_{sc} + X_{rac} J_{rs} \dot{X}_{sb} + X_{ra} J_{rs} \dot{X}_{sbc}. \tag{55}$$

Introducing Q-P notation in equation (55) yields the constraint relation

$$\begin{aligned} v_i P_{iabc} = {} & \eta_i Q_{iabc} + Q_{iab} \dot{P}_{ic} - P_{iab} \dot{Q}_{ic} + Q_{iac} \dot{P}_{ib} - P_{iac} \dot{Q}_{ib} \\ & + Q_{ia} \dot{P}_{ibc} - P_{ia} \dot{Q}_{ibc}. \end{aligned} \tag{56}$$

In the situation with two paraxial ray parameters, the lowercase indices a, b, and c are replaced by their corresponding uppercase versions. The constraint relation (56) can then be rephrased in terms of second- and third-order derivatives of traveltime,

$$\begin{aligned} v_i P_{iABC} = {} & \eta_i Q_{iABC} + \dot{M}_{ij} \, (Q_{iA} Q_{jBC} + Q_{iB} Q_{jAC} + Q_{iC} Q_{jAB}) \\ & + \dot{M}_{ijk} \, Q_{iA} Q_{jB} Q_{kC}. \end{aligned} \tag{57}$$

6 INITIAL CONDITIONS

To be able to start the integration operations described above we need initial conditions.

At the initial point of the ray Ω, for which the time is $\tau = \tau_0$, we denote the position vector as $\mathbf{x} = \hat{\mathbf{x}}(\tau_0)$ and the slowness vector as $\mathbf{p} = \hat{\mathbf{p}}(\tau_0)$. It is necessary to specify the phase-space perturbation derivatives $X_{ra}(\tau_0)$, $X_{rab}(\tau_0)$, $X_{rabc}(\tau_0), \ldots$ up to the highest order under consideration in the system of Hamilton-Jacobi perturbation equations.

We limit our discussion of initial conditions to those prescribed by two paraxial ray parameters γ_A, $A = 1, 2$. In this respect, two cases are of particular interest, i) the point source situation where the initial wavefront is degenerated and coincides with the source point, and ii) the plane-wave situation where the initial wavefront is a plane Π normal to the direction of the slowness vector $\hat{\mathbf{p}}(\tau_0)$.

To aid the setup of initial conditions, we introduce two linearly independent vectors $\mathbf{e}_1$ and $\mathbf{e}_2$ in the plane Π. Except for the requirements of linear independence and confinement

to the plane Π, the orientation of $\mathbf{e}_1$ and $\mathbf{e}_2$ is arbitrary. The components of $\mathbf{e}_1$ and $\mathbf{e}_2$ form the 3×2 matrix $\boldsymbol{\mathcal{E}} = \{\mathcal{E}_{iM}\}$. We establish a 3×3 matrix $\mathbf{H} = \{H_{ij}\}$ so that

$$\mathbf{H} \;=\; \left[\begin{array}{cc} \boldsymbol{\mathcal{E}} & \mathbf{v} \end{array} \right]. \tag{58}$$

The inverse $\mathbf{H}^\dagger = \mathbf{H}^{-1}$ may then be expressed as

$$\mathbf{H}^{-1} \;=\; \left[\begin{array}{c} \boldsymbol{\mathcal{F}}^T \\ \mathbf{p}^T \end{array} \right]. \tag{59}$$

If $\mathbf{e}_1$ and $\mathbf{e}_2$ are chosen orthonormal, one will be able to compute $\boldsymbol{\mathcal{F}}$ from the relation

$$\mathcal{F}_{iM} \;=\; [\delta_{ij} - p_i\, v_j]\; \mathcal{E}_{jM} \;=\; \alpha_{ij}\, \mathcal{E}_{jM}, \tag{60}$$

where all quantities belong to $\tau = \tau_0$. The quantity α_{ij} represents a projection operator with respect to the wave-propagation metric tensor (Hanyga 1982; Klimeš 2006). If $\mathbf{e}_1$ and $\mathbf{e}_2$ are not orthonormal, we compute $\boldsymbol{\mathcal{F}}$ from equation (59), so that

$$\mathcal{F}_{iM} \;=\; H^\dagger_{Mi}. \tag{61}$$

6.1 Point source

For a point source, the two ray parameters γ_A will be parametrizing the slowness vectors of rays starting out from that point. Obviously, the location x_i of a point on the (degenerated) source wavefront will be insensitive to any value of the parameters γ_A. As a consequence, all position perturbation derivatives on Ω are zero at the source point,

$$Q_{iA} = \frac{\partial x_i}{\partial \gamma_A} = 0, \quad Q_{iAB} = \frac{\partial^2 x_i}{\partial \gamma_A \partial \gamma_B} = 0, \quad Q_{iABC} = \frac{\partial^3 x_i}{\partial \gamma_A \partial \gamma_B \partial \gamma_C} = 0, \quad \text{etc.} \tag{62}$$

We define here the two ray parameters γ_A at the source point by

$$\gamma_A \;=\; \mathcal{E}_{iA}\; [p_i - \hat{p}_i(\tau_0)]\,. \tag{63}$$

It is remarked that other definitions are possible, for example, one may let the parameters γ_A be Euler angles. The parameters γ_A in equation (63) represent a projection of the slowness vector perturbation onto the coordinates corresponding to the vectors $\mathbf{e}_1$ and $\mathbf{e}_2$. One important notice in this context is that the three components of vector $\mathbf{p}$ are constrained, as they have to satisfy the Hamilton-Jacobi equation.

From equation (63) it follows that

$$\mathcal{E}_{iM}\, \frac{\partial p_i}{\partial \gamma_A}(\boldsymbol{\gamma}, \tau_0) \;=\; \delta_{MA}. \tag{64}$$

Moreover, the combination of constraint relation (49) and the first initial condition in equation (62) gives

$$v_i(\tau_0)\; P_{iA}(\tau_0) \;=\; 0. \tag{65}$$

Then, solving the system of equations (64)–(65) for $P_{iA}(\tau_0)$ yields at the initial point

$$P_{iA} \;=\; \mathcal{F}_{iA}, \tag{66}$$

where $\mathcal{F}_{iA}$ is given by equation (60) or (61).

To obtain $P_{iAB}(\tau_0)$, differentiate equation (64) further,

$$\mathcal{E}_{iM}\,\frac{\partial^2 p_i}{\partial\gamma_A\partial\gamma_B}(\boldsymbol{\gamma},\tau_0) \;=\; 0. \tag{67}$$

Also, we combine constraint relation (56) with initial conditions (62),

$$v_i(\tau_0)\; P_{iAB}(\tau_0) \;=\; -P_{iA}(\tau_0)\,\dot{Q}_{iB}(\tau_0). \tag{68}$$

Here, the time derivative on the right-hand side is given by the standard Hamilton-Jacobi perturbation equations (18). We solve equations (67)–(68) for $P_{iAB}(\tau_0)$, which yields

$$P_{iAB} \;=\; -p_i\,\mathcal{F}_{mA}\,\mathcal{F}_{nB}\,V_{mn}. \tag{69}$$

where all quantities belong to the initial point.

With values corresponding to a point source the constraint relation (56) becomes

$$v_j P_{jABC} \;=\; -P_{jA}\dot{Q}_{jBC} - P_{jAB}\dot{Q}_{jC} - P_{jAC}\dot{Q}_{jB}. \tag{70}$$

Applying equation (69), we obtain

$$\begin{aligned}\dot{Q}_{jBC} &= V_{jk}P_{kBC} + V_{jmn}P_{mB}P_{nC}\\ &= -V_{jk}p_k\mathcal{F}_{mB}\mathcal{F}_{nC}V_{mn} + V_{jmn}\mathcal{F}_{mB}\mathcal{F}_{nC}\\ &= -v_j\mathcal{F}_{mB}\mathcal{F}_{nC}V_{mn} + V_{jmn}\mathcal{F}_{mB}\mathcal{F}_{nC},\end{aligned} \tag{71}$$

where V_{jmn} is the tensor of third-order partial derivatives of the Hamiltonian with respect to slowness components, evaluated on the reference ray. Using equations (66), (69), and (71) in (70) then yields

$$v_j\,P_{jABC} \;=\; -V_{jmn}\mathcal{F}_{jA}\mathcal{F}_{mB}\mathcal{F}_{nC}. \tag{72}$$

Since equation (67) in addition implies that $\mathcal{E}_{iM}P_{iABC} = 0$, it follows that the initial condition for P_{iABC} is

$$P_{iABC} \;=\; -p_i V_{jmn}\mathcal{F}_{jA}\mathcal{F}_{mB}\mathcal{F}_{nC}. \tag{73}$$

If the Hamiltonian is a polynomial function of second degree in the slowness components, we have $V_{jmn} = 0$, and hence $P_{iABC} = 0$.

6.2 Plane-wave source

For a plane-wave source the two ray parameters γ_A may represent any pair of coordinates in the initial wavefront plane, Π. We choose here specifically these coordinates in the directions of the vectors $\mathbf{e}_1$ and $\mathbf{e}_2$ introduced earlier, such that $\partial\mathbf{x}/\partial\gamma_1 = \mathbf{e}_1$ and $\partial\mathbf{x}/\partial\gamma_2 = \mathbf{e}_2$ on Ω; hence,

$$\frac{\partial x_i}{\partial \gamma_A}(\hat{\boldsymbol{\gamma}}, \tau_0) \;=\; \mathcal{E}_{iA}. \tag{74}$$

Since our choice of plane-wave ray parameters γ_A is connected with the matrix $\boldsymbol{\mathcal{E}}$, the matrix $\boldsymbol{\mathcal{F}}$ in equation (59) will also relate to these ray parameters. The connection is simply

$$\mathcal{F}_{iA} \;=\; \frac{\partial \gamma_A}{\partial x_i}, \tag{75}$$

where $\gamma_A = \gamma_A(\mathbf{x})$, see equation (29), and where the derivative is taken at the source point on Ω. In view of equation (75) we find it natural to define the plane-wave ray parameters by the linear expression

$$\gamma_A \;=\; \mathcal{F}_{iA}\,[x_i - \hat{x}_i(\tau_0)]\,. \tag{76}$$

The following relations must then be satisfied along the plane Π,

$$\mathcal{F}_{iA}\,\frac{\partial x_i}{\partial \gamma_B}(\boldsymbol{\gamma}, \tau_0) \;=\; \delta_{AB}, \qquad \mathcal{E}_{iM}\,p_i(\boldsymbol{\gamma}, \tau_0) \;=\; 0, \tag{77}$$

Equation (74) readily yields the initial conditions

$$Q_{iA} \;=\; \mathcal{E}_{iA}, \qquad Q_{iAB} \;=\; 0, \qquad Q_{iABC} \;=\; 0. \tag{78}$$

Also, repeated differentiation of the last sub-equation in (77) with respect to γ_A gives

$$\mathcal{E}_{iM}\,P_{iA} \;=\; 0, \qquad \mathcal{E}_{iM}\,P_{iAB} \;=\; 0, \qquad \mathcal{E}_{iM}\,P_{iABC} \;=\; 0. \tag{79}$$

To obtain P_{iA} we use equation (79) and also invoke the constraint relation (49),

$$v_i P_{iA} \;=\; \eta_i Q_{iA}. \tag{80}$$

In combination, equations (79) and (80) yield the initial condition

$$P_{iA} \;=\; p_i\,\eta_j\,\mathcal{E}_{jA}. \tag{81}$$

Proceeding to compute P_{iAB}, we take constraint relation (53) with $Q_{iA} = \mathcal{E}_{iA}$ and $Q_{mAB} = 0$, as prescribed by initial conditions (78),

$$v_m P_{mAB} \;=\; Q_{mA}\dot{P}_{mB} - P_{mA}\dot{Q}_{mB}. \tag{82}$$

Using the standard Hamilton-Jacobi perturbation equations then gives

$$v_m P_{mAB} \;=\; (-U_{ij} + 3\eta_i\eta_j)\mathcal{E}_{iA}\mathcal{E}_{jB}. \tag{83}$$

The combination of the middle sub-equation (79) with (83) therefore yields

$$P_{mAB} \;=\; p_m\,[-U_{ij}+3\eta_i\,\eta_j]\;\mathcal{E}_{iA}\,\mathcal{E}_{jB}. \tag{84}$$

For the initial plane wavefront the constraint relation (56) can be formulated as (Appendix C)

$$\begin{aligned} v_m\,P_{mABC} &= Q_{mA}\dot{P}_{mBC}-P_{mA}\dot{Q}_{mBC}-P_{mAB}\dot{Q}_{mC}-P_{mAC}\dot{Q}_{mB} \\ &= (15\eta_i\eta_j\eta_k-3\eta_iU_{jk}-3\eta_jU_{ik}-3\eta_kU_{ij}-U_{ijk})\mathcal{E}_{iA}\mathcal{E}_{jB}\mathcal{E}_{kC}. \end{aligned} \tag{85}$$

Here, the tensor U_{ijk} represents the third-order derivatives of the Hamiltonian with respect to position components, evaluated on the reference ray. By combining the last sub-equation in (79) with (85) we obtain the initial condition

$$P_{mABC} \;=\; p_m(15\eta_i\eta_j\eta_k-3\eta_iU_{jk}-3\eta_jU_{ik}-3\eta_kU_{ij}-U_{ijk})\mathcal{E}_{iA}\mathcal{E}_{jB}\mathcal{E}_{kC}. \tag{86}$$

7 PARAXIAL EXTRAPOLATION

We describe extrapolation of geometrical spreading and traveltime away from the reference ray, Ω. The ray Ω is specified by paraxial ray parameters $\gamma_A=\gamma_{A0},\ A=1,2$, and it includes a source point, $\mathbf{x}=\mathbf{s}_0$, and a reference receiver point, $\mathbf{x}=\mathbf{r}_0$. The traveltime at $\mathbf{r}_0$ is $\tau=\tau_0^R=\tau(\mathbf{r}_0)$.

7.1 Extrapolation of geometrical spreading

In the neighbourhood of the reference receiver point $\mathbf{x}=\mathbf{r}_0$ we consider the 3×3 geometrical spreading matrix $\widehat{\mathbf{Q}}$ to be a function of the receiver position, $\mathbf{x}=\mathbf{r}$, while the source position is kept fixed. A Taylor-series expansion of $\widehat{\mathbf{Q}}$ in $\Delta\mathbf{r}=\mathbf{r}-\mathbf{r}_0$ reads

$$\begin{aligned} Q_{ia}(\mathbf{r},\mathbf{s}_0) &= Q_{ia}(\mathbf{r}_0,\mathbf{s}_0)\;+\;\frac{\partial Q_{ia}}{\partial r_k}(\mathbf{r}_0,\mathbf{s}_0)\,\Delta r_k\;+\;\frac{1}{2}\frac{\partial^2 Q_{ia}}{\partial r_k\partial r_l}(\mathbf{r}_0,\mathbf{s}_0)\,\Delta r_k\Delta r_l \\ &\quad+\frac{1}{6}\frac{\partial^3 Q_{ia}}{\partial r_k\partial r_l\partial r_m}(\mathbf{r}_0,\mathbf{s}_0)\,\Delta r_k\Delta r_l\Delta r_m+\ldots \end{aligned} \tag{87}$$

with the first three sets of derivatives given by

$$\frac{\partial Q_{ia}}{\partial r_k} \;=\; \frac{\partial^2 r_i}{\partial\gamma_a\partial\gamma_b}\frac{\partial\gamma_b}{\partial r_k} \;=\; Q_{iab}\,Q^{\dagger}_{bk}, \tag{88}$$

$$\begin{aligned} \frac{\partial^2 Q_{ia}}{\partial r_k\partial r_l} &= \frac{\partial^3 r_i}{\partial\gamma_a\partial\gamma_b\partial\gamma_c}\frac{\partial\gamma_b}{\partial r_k}\frac{\partial\gamma_c}{\partial r_l}\;+\;\frac{\partial^2 r_i}{\partial\gamma_a\partial\gamma_b}\frac{\partial^2\gamma_b}{\partial r_k\partial r_l} \\ &= Q_{iabc}\,Q^{\dagger}_{bk}\,Q^{\dagger}_{cl}\;+\;Q_{iab}\,Q^{\dagger}_{bkl}, \end{aligned} \tag{89}$$

$$\begin{aligned}\frac{\partial^3 Q_{ia}}{\partial r_k \partial r_l \partial r_m} &= \frac{\partial^4 r_i}{\partial\gamma_a \partial\gamma_b \partial\gamma_c \partial\gamma_d}\frac{\partial\gamma_b}{\partial r_k}\frac{\partial\gamma_c}{\partial r_l}\frac{\partial\gamma_d}{\partial r_m} \\ &\quad + \frac{\partial^3 r_i}{\partial\gamma_a \partial\gamma_b \partial\gamma_c}\left(\frac{\partial\gamma_b}{\partial r_k}\frac{\partial^2\gamma_c}{\partial r_l \partial r_m} + \frac{\partial\gamma_b}{\partial r_l}\frac{\partial^2\gamma_c}{\partial r_k \partial r_m}\right) + \frac{\partial^2 r_i}{\partial\gamma_a \partial\gamma_b}\frac{\partial^3\gamma_b}{\partial r_k \partial r_l \partial r_m} \\ &= Q_{iabcd}\, Q^\dagger_{bk}\, Q^\dagger_{cl}\, Q^\dagger_{dm} + Q_{iabc}\left(Q^\dagger_{bk}\, Q^\dagger_{clm} + Q^\dagger_{bl}\, Q^\dagger_{ckm}\right) + Q_{iab}\, Q^\dagger_{bklm}. \quad (90)\end{aligned}$$

We see that a first-order expansion of matrix $\{Q_{ia}\}$ relies on second-order perturbation derivatives Q_{iab}, a second order expansion of $\{Q_{ia}\}$ relies on third-order perturbation derivatives Q_{iabc}, and so forth. The derivatives of the transformation from Cartesian coordinates to ray coordinates, i.e., the quantities $Q^\dagger_{bk}$, $Q^\dagger_{bkl}$, $Q^\dagger_{bklm}\ldots$, can be obtained by repeated differentiation of equation (B.4).

It is assumed that the dynamic ray tracing is subject to point-source initial conditions at the point $\mathbf{s}_0$. The relative geometrical spreading for a paraxial ray from $\mathbf{s}_0$ to $\mathbf{r}$ can then be computed using

$$\mathcal{L}(\mathbf{r},\mathbf{s}_0) = \left[\frac{1}{c(\mathbf{r})}\det\{Q_{ia}(\mathbf{r},\mathbf{s}_0)\}\right]^{1/2}, \quad (91)$$

where $c(\mathbf{r})$ is the phase velocity of the paraxial ray evaluated at the position $\mathbf{r}$.

7.2 Extrapolation of traveltime

Consider the traveltime function $T(\mathbf{r},\mathbf{s}_0) = \tau(\mathbf{r})$ corresponding to a fixed source point at $\mathbf{x} = \mathbf{s}_0$. We write a Taylor expansion of T in $\Delta\mathbf{r}$,

$$\begin{aligned}T(\mathbf{r},\mathbf{s}_0) &= \tau_0^R + p_k\,\Delta r_k + \frac{1}{2}M_{kl}\,\Delta r_k \Delta r_l \\ &\quad + \frac{1}{6}M_{klm}\,\Delta r_k \Delta r_l \Delta r_m + \frac{1}{24}M_{klmn}\,\Delta r_k \Delta r_l \Delta r_m \Delta r_n + \ldots, \quad (92)\end{aligned}$$

where all the coefficients are evaluated at $\mathbf{r}_0$.

The 3×3 matrix of second derivatives of traveltime, $\mathbf{M}$, can be computed using equation (33). The latter is restated here as

$$M_{ij}\, Q_{ja} = P_{ia}, \quad (93)$$

where all indices run from 1 to 3. Differentiating equation (93) twice with respect to the ray coordinates yields,

$$M_{ijk}\, Q_{ja}\, Q_{kb} = P_{iab} - M_{ij}\, Q_{jab}, \quad (94)$$

$$\begin{aligned}M_{ijkl}\, Q_{ja}\, Q_{kb}\, Q_{lc} &= P_{iabc} \\ &\quad - M_{ijk}\,(Q_{ja}\, Q_{kbc} + Q_{jb}\, Q_{kac} + Q_{jc}\, Q_{kab}) - M_{ij}\, Q_{jabc}. \quad (95)\end{aligned}$$

When the right-hand sides of equations (93)–(95) have been evaluated, we obtain explicit

expressions for the second-, third- and fourth order derivatives of traveltime after multiplying by the relevant number of (inverse) matrices, $\{Q^{\dagger}_{aj}\}$.

To evaluate the right-hand side of (94) we need to know M_{ij}, which is precomputed using (93). In addition, we need Q_{iAB}, P_{iAB}, $\dot{Q}_{iA}$, $\dot{P}_{iA}$, $\dot{v}_i$, and $\dot{\eta}_i$. To evaluate the right-hand side of (95) we will also need M_{ijk}, precomputed using (94), as well as Q_{iABC}, P_{iABC}, $\dot{Q}_{iAB}$, $\dot{P}_{iAB}$, $\ddot{Q}_{iA}$, $\ddot{P}_{iA}$, $\ddot{v}_i$, and $\ddot{\eta}_i$. The temporal derivatives $\dot{Q}_{iA}$, $\dot{P}_{iA}$, $\dot{Q}_{iAB}$, and $\dot{P}_{iAB}$ can be readily obtained from the relevant system of differential equations given in the main text. The derivatives $\ddot{Q}_{iA}$, $\ddot{P}_{iA}$, $\dot{v}_i$, $\dot{\eta}_i$, $\ddot{v}_i$, and $\ddot{\eta}_i$ can be obtained after temporal differentiation of such equations.

In some situations it can be useful to do a Taylor expansion of squared traveltime rather than of the traveltime itself, as the expansion of $T^2(\mathbf{r}, \mathbf{s}_0)$ to second order in $\Delta\mathbf{r}$ is exact for waves from a point source in an isotropic homogeneous medium. For underlying theory and numerical examples, see Ursin (1982); Gjøystdal et al. (1984). Extrapolation of squared traveltime may be highly appropriate also for a transversely isotropic medium with a vertical axis of symmetry. For details on this matter, see Alkhalifah & Tsvankin (1995) and Tsvankin (2013).

8 HAMILTONIANS FOR P AND S WAVES IN ANISOTROPIC HETEROGENEOUS MEDIA

Up to this point, the theory has been described with the Hamiltonian appearing as a black box. In this section, we elaborate on specific Hamiltonians related to P and S waves in anisotropic heterogeneous media.

8.1 Arbitrary anisotropy

The Christoffel matrix $\mathbf{\Gamma}$, as defined e.g. in Červený (2001), equation (2.2.19), is of size 3×3 and has the components

$$\Gamma_{ik}(\mathbf{x}, \mathbf{p}) = a_{ijkl}(\mathbf{x})\, p_j p_l. \tag{96}$$

Here, a_{ijkl} is the tensor of density-normalized elastic moduli. The Christoffel matrix has three real eigenvalues and three corresponding mutually orthogonal eigenvectors. One selected eigenvalue and its associated eigenvector are denoted, respectively, by the symbols G and $\mathbf{g}$. The eigenvalue G corresponds to an elementary P or S wave with polarization vector $\mathbf{g}$.

The eigenvalues of matrix $\mathbf{\Gamma}$ satisfy the characteristic equation

$$\det(\mathbf{\Gamma} - G\mathbf{I}) = 0; \tag{97}$$

here. $\mathbf{I}$ is the 3×3 identity matrix. Equation (97) represents a third-order polynomial in G,

$$G^3 - PG^2 + QG - R = 0, \tag{98}$$

where the quantities P, Q, and R are invariants of $\mathbf{\Gamma}$,

$$P = \mathrm{tr}\mathbf{\Gamma}, \quad Q = \mathrm{tr}(\mathrm{cof}\mathbf{\Gamma}), \quad R = \det \mathbf{\Gamma}. \tag{99}$$

We note that P, Q, and R are scalar functions in phase space, and they are homogeneous of degree two (P), four (Q), and six (R) in the slowness components, p_i. The function G is homogeneous of degree two p_i.

For a given wave mode and a given point $\mathbf{x}$, we get an exact description of the relevant slowness-surface sheet if the eigenvalue function G is subject to the constraint $G(\mathbf{w}) = 1$. On the other hand, our Hamiltonian $\mathcal{H}$ satisfies the Hamilton-Jacobi equation $\mathcal{H} = 1/2$. Hence, to ensure consistency with the slowness surface it is natural to express $\mathcal{H}$ in terms of G, such that

$$\mathcal{H}(\mathbf{w}) \;=\; \frac{1}{2}\, G(\mathbf{w}). \tag{100}$$

In the case of arbitrary anisotropy, derivatives of $\mathcal{H}$ are obtained by differentiation of equations (98) and (100), followed by setting $G = 1$.

We remark that for some applications of ray perturbation theory (see, e.g., Klimeš, 2002b; Červený & Klimeš, 2009) it may be useful to redefine the Hamiltonian to

$$\mathcal{H}(\mathbf{w}) \;=\; \frac{1}{\mathcal{N}}\, [G(\mathbf{w})]^{\mathcal{N}/2}\,, \tag{101}$$

where $\mathcal{N}$ is a nonzero scalar. Such a redefinition will only affect the non-eikonal solution to dynamic ray tracing; the other fundamental solutions are unaffected.

8.2 Partial factoring of the characteristic equation by polarization

For particular anisotropic symmetries, e.g. transversely isotropic media, one can utilize a partial factoring of the characteristic equation (98) by polarization. One of the elementary S waves is then SH polarized, meaning that the polarization vector is confined to the (locally) horizontal plane. The polarization vectors of the two other elementary waves, P and SV, form a (locally) vertical plane. The partial factoring is stated

$$(G^2 - P^{PSV} G + R^{PSV})(G - G^{SH}) = 0. \tag{102}$$

In this situation we get a specific equation for the Hamiltonian of the SH-polarized wave,

$$\mathcal{H} = \frac{1}{2} G^{SH}. \tag{103}$$

with slowness-surface distance function The eigenvalue function G^{SH} is homogeneous of degree two in the slowness components, and the slowness sheet for the SH wave is elliptical.

Equation (102) further yields another, common, equation for the P- and SV-polarized waves,

$$G^2 - P^{PSV} G + R^{PSV} = 0. \tag{104}$$

The functions P^{PSV} and R^{PSV} are homogeneous of degree two and four in the slowness components.

For an SH wave, derivatives of $\mathcal{H}$ in phase space are obtained by differentiating equation (103). For a P or SV wave, we differentiate equations (100) and (104), followed by setting $G = 1$.

8.3 Full factoring of the characteristic equation by polarization

Consider a further factoring of equation (102) so that

$$(G - G^P)(G - G^{SV})(G - G^{SH}) = 0. \tag{105}$$

This yields the following possibilities for the Hamiltonian,

$$\mathcal{H} = \frac{1}{2} G^P, \qquad \mathcal{H} = \frac{1}{2} G^{SV}, \qquad \mathcal{H} = \frac{1}{2} G^{SH}. \tag{106}$$

The eigenvalue functions $G^P(\mathbf{w})$, $G^{SV}(\mathbf{w})$, and $G^{SH}(\mathbf{w})$ are all homogeneous of second degree in the slowness components. The P- and SH-wave slowness sheets are elliptical; the SV-wave slowness sheet is spherical.

To obtain derivatives of the Hamiltonian $\mathcal{H}$, we differentiate the relevant eigenvalue function in equation (106).

9 NUMERICAL EXAMPLES

We have performed numerical tests of the above described higher-order approaches to dynamic ray tracing in Cartesian coordinates, using three related 3D heterogeneous models. All the simulation examples are for P waves. In this section the spatial coordinates of the models are referred to as (x, y, z).

9.1 Model ISO

The first model, Model ISO, is adopted from Iversen & Tygel (2008)— it is isotropic and includes a gentle anticline structure (Fig. 1). However, in the implementation of higher-order

dynamic ray tracing we use a quintic (fifth-order) B-spline representation (e.g., Farin et al., 2002) to ensure C^4 continuity of the volumetric medium parameter functions. As a consequence, the P-wave velocity field appears here in a somewhat smoother form than in Iversen & Tygel (2008). The ratio of S-wave to P-wave velocity is constant = 0.5. Data for numerical comparisons is obtained using conventional P-wave kinematic and dynamic ray tracing from a source point at depth $z = 4$ km to receivers in the plane at zero depth. Fig. 1 shows a sub-selection of rays (black) for receivers along the line $y = 5$ km. The ray (grey) arriving at the receiver location (7, 5, 0) km is taken as a reference ray for higher-order dynamic ray tracing computations.

Fig. 2 shows the computed traveltime data (top) and geometrical spreading data (bottom). Geometrical spreading was computed using equation (91). As ray parameters γ_A in that equation we used the two horizontal components of the slowness vector at the source point.

Our results are shown as error curves for the extrapolated traveltime (Fig. 3) and the extrapolated geometrical spreading (Fig. 4). The computed error curves belong to a line of constant y (= 5 km) and a line of constant x (= 7 km). We refer to the lateral distance between a receiver and the reference ray as the *paraxial distance*. In the cross sections $y = 5$ and $x = 7$ (km) the maximum paraxial distance is 3 km.

For traveltime extrapolation, we observe that second-order extrapolation of squared traveltime (dashed blue) yields a very good result. The maximum relative errors at 3 km paraxial distance are around 0.15%. For heterogeneous media such a good result is not obvious (Gjøystdal et al. 1984). In the current test, however, the heterogeneities are moderate. We note that the results for fourth-order extrapolation of traveltime (magenta) and squared traveltime (dashed magenta) are also very good. The range of relative errors for the latter approach is 0-0.3%.

Concerning extrapolation of geometrical spreading, a striking observation is that the extrapolation function needs to be at least third order in the perturbation derivatives, in order to be appropriate at large paraxial distances. The relative errors obtained for the third-order approach (magenta) are below 1% for paraxial distances 0–1.5 km and below 5% for paraxial distances 1.5–3 km.

9.2 Model VEL

The second model, Model VEL, differs from Model ISO only in one respect— we have introduced elliptic anisotropy related to a vertical axis of symmetry. The anisotropy was defined to be constant, with Thomsen's (1986) parameters specified as $\epsilon = \delta = 0.2$. Since we consider

P-wave simulation only, the value of Thomsen's parameter γ (not to be confused with ray parameters) does not affect our computations.

To get an impression of the effect of introducing strong elliptic anisotropy we can compare Figs. 2 and 5. We note a decrease in traveltime at large lateral distances from the reference ray, and also a general increase in the values of geometrical spreading.

Figs. 6 and 7 show the same type of error curves as was given for Model ISO (Figs. 3 and 4). Extrapolation of squared traveltime to second order (dashed blue) yields also for Model VEL an excellent result. The reason is twofold— the heterogeneities are moderate and the anellipticity effect is zero. For a corresponding homogeneous model the fourth-order term of the extrapolation function for squared traveltime would have vanished completely (Alkhalifah & Tsvankin 1995). The results for fourth-order extrapolation of traveltime (magenta) and squared traveltime (dashed magenta) are also very good. We note that the results for second-order extrapolation of traveltime (blue) and third-order extrapolation of traveltime are significantly better than in the isotropic case. Third-order extrapolation of geometrical spreading (magenta) has the same level of relative accuracy as for the isotropic model, i.e., less than 1% / 5% for paraxial distance ranges, respectively, 0–1.5 km / 1.5–3 km.

9.3 Model VTI

In the third model, Model VTI, the anisotropy is transversely isotropic (hexagonal) relative to a vertical axis of symmetry. We have introduced anellipticity in the slowness surface by the parameter setting $\epsilon = 0.3$, $\delta = 0.1$. The parameters are constant throughout the model, so the anellipticity is invariant.

By comparing Fig. 5 for Model VEL with Fig. 8, we see that the change in traveltime is quite minor, while geometrical spreading has substantial changes at large lateral offsets with respect to the reference ray.

Figs. 9 and 10 show curves of relatives errors in traveltime and geometrical spreading. They are to be compared to the corresponding Figs. 3–4 (for Model ISO) and 6–7 (for Model VEL). We observe that it is now harder to get a good extrapolation result in the full range of paraxial distances (3 km). When using fourth-order extrapolation of squared traveltime, the errors are below 0.025% within a paraxial distance of 2 km. For third-order extrapolation of geometrical spreading, errors are below 1% within 1 km paraxial distance.

10 DISCUSSION AND CONCLUSIONS

We give a brief discussion on the connections to differential geometry, followed by our concluding remarks.

The theory derived in this paper has important connections to differential geometry— in particular to the Riemannian and Finslerian geometry systems (see, e.g., Shen, 2001; Bao et al., 2012). Any Riemannian, Finslerian, or similar geometrical structure can be completely described by distances. In the propagation of elastic waves distance is naturally measured in traveltime: the distance between two points is the shortest time it takes for a wave to go from one point to the other. By Fermat's principle elastic waves travel along geodesics (rays). Locally, the geodesics represent length-minimizing curves of the geometrical structure under consideration.

The elastic geometry of P waves in anisotropic media is Finsler geometry, as observed by Antonelli et al. (2003). If the anisotropy is elliptical, then the Finsler geometry simplifies to Riemannian geometry. For anisotropy of lower order than elliptic, non-Riemannian geometric features are intrinsic properties of the medium. Leading-order variations from a reference ray can be adequately described by elliptic anisotropy, and similarly, a Finsler geometry has a canonical Riemannian metric along a reference geodesic. Higher-order variations require a Finsler treatment— elliptic approximations are insufficient.

To gain access to the powerful tools of differential geometry, it is reasonable to rephrase the study of elastic waves in a geometrical framework. Writing equations in terms of coordinate invariant geometrical quantities simplifies the structure significantly. Many extra terms in calculations in anisotropic heterogeneous media may be viewed as a symptom of computing in coordinates rather than invariantly. For example, the geometric counterpart of the Q-P quantities is a Jacobi field and its covariant derivative; for details on the geometrical aspects, see Paternain (2012). In the equation of motion of the geometrical variant, similar to equation (18), the diagonal blocks are automatically zero and the the top-right block is the identity. All geometrical information is packed into the curvature operator appearing as the lower left block. It is our intention to elaborate on these connections between differential geometry and seismology in future work.

A key motivation behind this paper is to contribute to better computational capabilities, with respect to accuracy as well as efficiency, for processes exploiting amplitude and/or phase properties of high-frequency Green's functions.

The starting point of the theory development is a Hamilton-Jacobi equation in Cartesian coordinates. Based on this fundamental equation, we first reviewed the standard approach to

dynamic ray tracing, by which first-order phase-space perturbation derivatives are continued along a reference ray. Thereafter, we developed a theoretical framework for computation of higher-order phase-space perturbation derivatives. Detailed results were exposed for the orders two and three in these derivatives.

We did numerical tests of higher-order dynamic ray tracing for three related 3D heterogeneous models— one isotropic, one elliptically anisotropic, and one transversely isotropic. The higher-order approach yields clear improvements of the paraxial extrapolation of traveltime and geometrical spreading, compared to results obtained using conventional dynamic ray tracing. One important observation is that the extrapolation function for geometrical spreading must be at least third order to be appropriate at large extrapolation distances.

The presented methodology opens possibilities for further research and development in several directions. So far we have only considered continuous models— for completeness it should also be possible to use models with interfaces. Furthermore, when concerning S waves in anisotropic media one should take into account Hamiltonians that honour both elementary S waves simultaneously, such that problems with S-wave singularities are circumvented. With higher-order perturbation derivatives available it should also be possible to formulate higher-order variants of Hamilton's two-point characteristic. Last, but not least, it would be of great interest to see the method developed for ray-centred coordinates, taking into account the connections to differential geometry outlined above.

ACKNOWLEDGEMENTS

Maarten V. de Hoop gratefully acknowledges support from the Simons Foundation under the MATH + X program, the National Science Foundation under grant DMS-1815143, and the corporate members of the Geo-Mathematical Group at Rice University. Teemu Saksala gratefully acknowledges support from the Simons Foundation under the MATH + X program. Joonas Ilmavirta has been supported by the Academy of Finland (decision 295853). Bjørn Ursin has received support from the Research Council of Norway through the ROSE project. Einar Iversen and Bjørn Ursin are grateful for being invited to meetings at Rice University. In this work we have used academic software licenses from MATLAB and NORSAR.

REFERENCES

Alkhalifah, T. & Tsvankin, I., 1995. Velocity analysis for transversely isotropic media, *Geophysics*, **60**(5), 1550–1566.

Antonelli, P., Rutz, S., & Slawinski, M., 2003. A geometrical foundation for seismic ray theory based on modern finsler geometry, in *Finsler and Lagrange Geometries*, pp. 17–54, Springer.

Bao, D., Chern, S.-S., & Shen, Z., 2012. *An introduction to Riemann-Finsler geometry*, vol. 200, Springer Science & Business Media.

Beylkin, G. & Burridge, R., 1990. Linearized inverse scattering problems in acoustics and elasticity, *Wave Motion*, **12**(1), 15 – 52.

Bleistein, N., Cohen, J. K., & Stockwell Jr., J. W., 2001. *Mathematics of Multidimensional Seismic Imaging, Migration, and Inversion*, Springer.

Bortfeld, R., 1989. Geometrical ray theory: Rays and traveltimes in seismic systems (second-order approximation of the traveltimes), *Geophysics*, **54**, 342–349.

Brandsberg-Dahl, S., de Hoop, M. V., & Ursin, B., 2003a. Focusing in dip and ava compensation on scatteringangle/azimuth common image gathers, *Geophysics*, **68**(1), 232–254.

Brandsberg-Dahl, S., Ursin, B., & de Hoop, M. V., 2003b. Seismic velocity analysis in the scattering angle/azimuth domain, *Geophysical Prospecting*, **51**(4), 295–314.

Cameron, M. K., Fomel, S., & Sethian, J. A., 2007. Seismic velocity estimation from time migration, *Inverse Problems*, **23**, 1329–1369.

Červený, V., 1972. Seismic rays and ray intensities in inhomogeneous anisotropic media, *Geophys. J. Roy. Astr. Soc.*, **29**, 1–13.

Červený, V. & Klimeš, L., 2009. Transformation relations for second derivatives of traveltime in anisotropic media, in *19th annual report of the Seismic Waves in Complex 3-D Structures (SW3D) consortium*, pp. 115–122, Department of Geophysics, Faculty of Mathematics and Physics, Charles University, Praha.

Červený, V. & Pšenčík, I., 2010. Gaussian beams in inhomogeneous anisotropic layered structures, *Geophysical Journal International*, **180**(2), 798–812.

Červený, V., Klimeš, L., & Pšenčík, I., 1984. Paraxial ray approximations in the computation of seismic wavefields in inhomogeneous media, *Geophysical Journal of the Royal Astronomical Society*, **79**, 89–104.

Červený, V., Iversen, E., & Pšenčík, I., 2012. Two-point paraxial traveltimes in an inhomogeneous anisotropic medium, *Geophysical Journal International*, **189**(3), 1597–1610.

Chapman, C. H., 2004. *Fundamentals of Seismic Wave Propagation*, Cambridge University Press.

de Hoop, M., Holman, S., Iversen, E., Lassas, M., & Ursin, B., 2014. Reconstruction of a Conformally Euclidean Metric from Local Boundary Diffraction Travel Times, *SIAM Journal on Mathematical Analysis*, **46**(6), 3705–3726.

de Hoop, M. V. & Bleistein, N., 1997. Generalized radon transform inversions for reflectivity in

anisotropic elastic media, *Inverse Problems*, **13**(3), 669.

de Hoop, M. V., Burridge, R., Spencer, C., & Miller, D., 1994. Generalized radon transform/amplitude versus angle (grt/ava) migration/inversion in anisotropic media, *Proc. SPIE*, **2301**, 15–27.

de Hoop, M. V., Smith, H., Uhlmann, G., & van der Hilst, R. D., 2009. Seismic imaging with the generalized radon transform: a curvelet transform perspective, *Inverse Problems*, **25**(2), 025005.

de Hoop, M. V., Holman, S. F., Iversen, E., Lassas, M., & Ursin, B., 2015. Recovering the isometry type of a riemannian manifold from local boundary diffraction travel times, *Journal de Mathmatiques Pures et Appliques*, **103**(3), 830 – 848.

de Hoop, M. V. d. & Uhlmann, G., 2006. Characterization and 'source-receiver' continuation of seismic reflection data, *Communications in Mathematical Physics*, **263**(1), 1–19.

Douma, H. & de Hoop, M. V., 2006. Explicit expressions for prestack map time migration in isotropic and VTI media and the applicability of map depth migration in heterogeneous anisotropic media, *Geophysics*, **71**(01), S13–S28.

Duchkov, A. A. & de Hoop, M. V., 2010. Extended isochron rays in prestack depth (map) migration, *Geophysics*, **75**(4), S139–S150.

Farin, G., Hoschek, J., & Kim, M.-S., 2002. *Handbook of computer aided geometric design*, Elsevier, Amsterdam.

Farra, V. & Madariaga, R., 1987. Seismic waveform modeling in heterogeneous media by ray perturbation theory, *Journal of Geophysical Research*, **92**, 2697–2712.

Foss, S.-K. & Ursin, B., 2004. 2.5d modelling, inversion and angle migration in anisotropic media, *Geophysical Prospecting*, **52**, 65–84.

Foss, S.-K., Ursin, B., & Sollid, A., 2004. A practical approach to pp seismic angle tomography, *Geophysical Prospecting*, **52**, 663–669.

Foss, S.-K., de Hoop, M. V., & Ursin, B., 2005. Linearized 2.5-dimensional parameter imaging inversion in anisotropic elastic media, *Geophysical Journal International*, **161**, 722–738.

Gjøystdal, H., Reinhardsen, J. E., & Ursin, B., 1984. Traveltime and wavefront curvature calculations in three-dimensional inhomogeneous layered media with curved interfaces, *Geophysics*, **49**, 1466–1494.

Goldin, S. V. & Duchkov, A. A., 2003. Seismic wave field in the vicinity of caustics and higher-order travel time derivatives, *Studia Geophysica et Geodaetica*, **47**, 521–544.

Hamilton, W. R., 1837. Third supplement to an essay on the theory of systems of rays, *Transactions of the Royal Irish Academy*, **17**, 1–144, read January 23, 1832, and October 22, 1832.

Hanyga, A., 1982. Dynamic ray tracing in an anisotropic medium, *Tectonophysics*, **90**, 243–251.

Hubral, P., 1977. Time migration - Some ray theoretical aspects, *Geophysical Prospecting*, **25**(04), 738–745.

Hubral, P., 1983. Computing true amplitude reflections in a laterally inhomogeneous earth, *Geophysics*, **48**, 1051–1062.

Hubral, P., Schleicher, J., & Tygel, M., 1992. Three-dimensional paraxial ray properties: – Basic relations, *Journal of Seismic Exploration*, **1**, 265–279.

Iversen, E., 2004a. The isochron ray in seismic modeling and imaging, *Geophysics*, **69**(4), 1053–1070.

Iversen, E., 2004b. Reformulated kinematic and dynamic ray tracing systems for arbitrarily anisotropic media, *Studia Geophysica et Geodaetica*, **48**, 1–20.

Iversen, E. & Gjøystdal, H., 1996. Event-oriented velocity estimation based on prestack data in time or depth domain, *Geophysical Prospecting*, **44**(4), 643–686.

Iversen, E. & Pšenčík, I., 2008. Ray tracing and inhomogeneous dynamic ray tracing for anisotropy specified in curvilinear coordinates, *Geophysical Journal International*, **174**, 316–330.

Iversen, E. & Tygel, M., 2008. Image-ray tracing for joint 3D seismic velocity estimation and time-to-depth conversion, *Geophysics*, **73**(3), P99–P114.

Iversen, E., Tygel, M., Ursin, B., & de Hoop, M. V., 2012. Kinematic time migration and demigration of reflections in pre-stack seismic data, *Geophysical Journal International*, **189**(3), 1635–1666.

Jäger, R., Mann, J., Höcht, G., & Hubral, P., 2001. Common-reflection-surface stack: Image and attributes, *Geophysics*, **66**(1), 97–109.

Klimeš, L., 1994. Transformations for dynamic ray tracing in anisotropic media, *Wave Motion*, **20**, 261–272.

Klimeš, L., 2006. Ray-centred coordinate systems in anisotropic media, *Studia Geophysica et Geodaetica*, **50**, 431–447.

Klimeš, L., 2002a. Relation of the wave-propagation metric tensor to the curvatures of the slowness and ray-velocity surfaces, *Studia Geophysica et Geodaetica*, **46**(3), 589–597.

Klimeš, L., 2002b. Second-order and higher-order perturbations of travel time in isotropic and anisotropic media, *Studia Geophysica et Geodetica*, **46**(2), 213–248.

Moser, T. J. & Červený, V., 2007. Paraxial ray methods for anisotropic inhomogeneous media, *Geophysical Prospecting*, **55**, 21–37.

Paternain, G. P., 2012. *Geodesic flows*, vol. 180, Springer Science & Business Media.

Rabbel, W., Bittner, R., & Gelchinsky, B., 1991. Seismic mapping of complex reflectors with the common-reflecting-element method (cre method), *Physics of the Earth and Planetary Interiors*, **67**(1), 200 – 210.

Schleicher, J., Tygel, M., & Hubral, P., 2007. *Seismic True-Amplitude Imaging*, Society of Exploration Geophysicists.

Shen, Z., 2001. *Lectures on Finsler geometry*, World Scientific.

Sollid, A. & Ursin, B., 2003. Scattering-angle migration of ocean-bottom seismic data in weakly anisotropic media, *Geophysics*, **68**(2), 641–655.

Stolk, C. & de Hoop, M., 2006. Seismic inverse scattering in the downward continuation approach, *Wave Motion*, **43**(7), 579–598.

Stolk, C. C. & de Hoop, M. V., 2002. Microlocal analysis of seismic inverse scattering in anisotropic

elastic media, *Communications on Pure and Applied Mathematics*, **55**(3), 261–301.

Thomsen, L., 1986. Weak elastic anisotropy, *Geophysics*, **51**, 1954–1966.

Tsvankin, I., 2013. *Seismic Signatures and Analysis of Reflection Data in Anisotropic Media, Third Edition*, Society of Exploration Geophysicists.

Tygel, M., Ursin, B., Iversen, E., & de Hoop, M. V., 2012. Estimation of geological dip and curvature from time-migrated zero-offset reflections in heterogeneous anisotropic media, *Geophysical Prospecting*, **60**(2), 201–216.

Ursin, B., 1982. Quadratic wavefront and travel time approximations in inhomogeneous layered media with curved interfaces, *Geophysics*, **47**, 1012–1021.

Ursin, B., 2004. Parameter inversion and angle migration in anisotropic elastic media, *Geophysics*, **69**, 1125–1142.

Červený, V., 2001. *Seismic Ray Theory*, Cambridge University Press.

Červený, V. & Moser, T. J., 2007. Ray propagator matrices in three-dimensional anisotropic inhomogeneous layered media, *Geophysical Journal International*, **168**, 593–604.

APPENDIX A: RELATIONS FOR DERIVATIVES OF THE HAMILTONIAN

The considered Hamiltonian $\mathcal{H}$ satisfies the relations

$$p_i \frac{\partial^2 \mathcal{H}}{\partial p_i \partial p_j} = \frac{\partial \mathcal{H}}{\partial p_j}, \qquad p_i \frac{\partial^2 \mathcal{H}}{\partial p_i \partial x_j} = 2 \frac{\partial \mathcal{H}}{\partial x_j}. \tag{A.1}$$

These relations hold on the reference ray, Ω, as well as in its vicinity.

For the third-order derivatives of $\mathcal{H}$ we have the following general relations,

$$p_i \frac{\partial^3 \mathcal{H}}{\partial p_i \partial x_j \partial x_k} = 2 \frac{\partial^2 \mathcal{H}}{\partial x_j \partial x_k}, \tag{A.2}$$

$$p_i \frac{\partial^3 \mathcal{H}}{\partial p_i \partial p_j \partial x_k} = \frac{\partial^2 \mathcal{H}}{\partial p_j \partial x_k}, \tag{A.3}$$

$$p_i p_j \frac{\partial^3 \mathcal{H}}{\partial p_i \partial p_j \partial x_k} = 2 \frac{\partial \mathcal{H}}{\partial x_k}, \tag{A.4}$$

It is important to note that $\mathcal{H}$ may have nonzero derivatives of order three and higher in the slowness components. In particular, it follows from equation (A.1) that the third- and fourth-order derivatives must satisfy

$$p_i \frac{\partial^3 \mathcal{H}}{\partial p_i \partial p_j \partial p_k} = 0 \tag{A.5}$$

and

$$p_i \frac{\partial^4 \mathcal{H}}{\partial p_i \partial p_j \partial p_k \partial p_l} = -\frac{\partial^3 \mathcal{H}}{\partial p_j \partial p_k \partial p_l}. \tag{A.6}$$

APPENDIX B: TWO-PARAMETRIC SYSTEM OF RAYS

Consider a ray-parameter space (γ_A) with dimension $N_\gamma = 2$, and the associated ray-coordinate system, $(\gamma_1, \gamma_2, \tau)$. In a local region around a point on the reference ray we assume that a one-to-one mapping exists between the Cartesian coordinates (x_1, x_2, x_3) and the ray coordinates $(\gamma_1, \gamma_2, \tau)$.

B1 First-order transformation between Cartesian coordinates and ray coordinates

To first order, the quantities on Ω describing the transformation from ray coordinates to Cartesian coordinates are

$$\frac{\partial x_i}{\partial \gamma_A} = Q_{iA}, \qquad \frac{\partial x_i}{\partial \tau} = v_i = Q_{i3}. \tag{B.1}$$

For the inverse transformation we use the functions $\gamma_A = \gamma_A(\mathbf{x})$ and $\tau = \tau(\mathbf{x})$, with the first-order derivatives

$$\frac{\partial \gamma_A}{\partial x_i} = Q^\dagger_{Ai}, \qquad \frac{\partial \tau}{\partial x_i} = p_i = Q^\dagger_{3i}. \tag{B.2}$$

The quantities in equations (B.1) and (B.2) form the 3×3 matrices

$$\widehat{\mathbf{Q}} = \begin{bmatrix} \mathbf{Q} & \mathbf{v} \end{bmatrix}, \qquad \widehat{\mathbf{Q}}^{-1} = \widehat{\mathbf{Q}}^\dagger = \begin{bmatrix} \mathbf{Q}^\dagger \\ \mathbf{p}^T \end{bmatrix}. \tag{B.3}$$

Based on the relations

$$Q^\dagger_{ai} Q_{ib} = \delta_{ab} \qquad Q_{ia} Q^\dagger_{aj} = \delta_{ij}, \tag{B.4}$$

we can list some intrinsic properties of the transformation between ray coordinates and Cartesian coordinates on Ω,

$$\begin{aligned} p_i Q_{iA} &= 0, \\ v_i Q^\dagger_{Ai} &= 0, \\ Q^\dagger_{Ai} Q_{iB} &= \delta_{AB}, \\ p_i v_i &= 1, \\ Q^\dagger_{Ai} Q_{jA} &= \alpha_{ij}, \end{aligned} \tag{B.5}$$

where α_{ij} is given by

$$\alpha_{ij} = \delta_{ij} - p_i v_j. \tag{B.6}$$

B2 Second-order derivatives of traveltime

Consider a specific traveltime function $\tau(\mathbf{x})$ which correspond to two paraxial ray parameters $\gamma_A(\mathbf{x})$, $A = 1, 2$. The first- and second-order derivatives of τ on Ω are

$$\frac{\partial \tau}{\partial x_i} = p_i, \tag{B.7}$$

$$\frac{\partial^2 \tau}{\partial x_i \partial x_j} = M_{ij}. \tag{B.8}$$

The quantities M_{ij} are forming the 3×3 matrix $\mathbf{M}$.

Using the chain rule for differentiation, we then obtain

$$\begin{aligned} \frac{\partial^2 \tau}{\partial x_i \partial x_j} &= \frac{\partial}{\partial x_j} \left\{ p_i \left[\gamma_A(\mathbf{x}), \tau(\mathbf{x}) \right] \right\} \\ &= \frac{\partial p_i}{\partial \gamma_A} \frac{\partial \gamma_A}{\partial x_j} + \frac{\partial p_i}{\partial \tau} \frac{\partial \tau}{\partial x_j}, \end{aligned}$$

and consequently,

$$M_{ij} = P_{iA}\, Q^{\dagger}_{Aj} + \eta_i\, p_j, \qquad \mathbf{M} = \mathbf{P}\, \mathbf{Q}^{\dagger} + \boldsymbol{\eta}\, \mathbf{p}^T. \tag{B.9}$$

The last relation describes how the 3×3 matrix of second derivatives of traveltime, $\mathbf{M}$, can be obtained from the 3×2 matrices $\mathbf{P}$ and $\mathbf{Q}$ computed using the (standard) Hamilton-Jacobi perturbation equations. The 2×3 matrix $\mathbf{Q}^{\dagger}$ is a sub-matrix of matrix $\widehat{\mathbf{Q}}^{-1}$ in equation (B.3).

APPENDIX C: CONSTRAINT RELATION FOR THIRD-ORDER PHASE-SPACE PERTURBATION DERIVATIVES: PLANE WAVEFRONT

Based on equation (56), the constraint relation for third-order phase-space perturbation derivatives and two ray parameters can be written

$$\begin{aligned} v_i P_{iABC} &= \eta_i Q_{iABC} + Q_{iA}\dot{P}_{iBC} - P_{iA}\dot{Q}_{iBC} \\ &\quad + Q_{iAB}\dot{P}_{iC} - P_{iAB}\dot{Q}_{iC} \\ &\quad + Q_{iAC}\dot{P}_{iB} - P_{iAC}\dot{Q}_{iB}. \end{aligned} \tag{C.1}$$

In this appendix we derive a special version of equation (C.1), pertaining specifically to a plane wavefront. On the way we use relations for the derivatives of the Hamiltonian given in Appendix A. It is convenient to use abbreviated forms for partial derivatives in these derivations, namely,

$$\partial_k^1 = \frac{\partial}{\partial x_k}, \qquad \partial_k^2 = \frac{\partial}{\partial p_k}, \tag{C.2}$$

and

$$\frac{\partial \mathcal{H}}{\partial x_k} = \mathcal{H}_{,k}^{,1}, \quad \frac{\partial \mathcal{H}}{\partial p_k} = \mathcal{H}_{,k}^{,2}, \quad \frac{\partial^2 \mathcal{H}}{\partial x_k \partial x_l} = \mathcal{H}_{,kl}^{,11}, \quad \frac{\partial^2 \mathcal{H}}{\partial x_k \partial p_l} = \mathcal{H}_{,kl}^{,12}, \quad \frac{\partial^2 \mathcal{H}}{\partial p_k \partial p_l} = \mathcal{H}_{,kl}^{,22}, \tag{C.3}$$

and so forth.

We find expressions for the various quantities on the right-hand side of equation (C.1). In particular, we can use the ODEs in equation (37) to obtain

$$\begin{aligned} \dot{Q}_{iBC} &= \mathcal{H}_{,mi}^{,12} Q_{mBC} + \mathcal{H}_{,im}^{,22} P_{mBC} \\ &\quad + Q_{mB}\,[Q_{nC}\,\partial_n^1 + P_{nC}\,\partial_n^2]\,\mathcal{H}_{,mi}^{,12} \\ &\quad + P_{mB}\,[Q_{nC}\,\partial_n^1 + P_{nC}\,\partial_n^2]\,\mathcal{H}_{,im}^{,22}, \end{aligned}$$

which yields

$$\begin{aligned} \dot{Q}_{iBC} &= \mathcal{H}_{,mi}^{,12} Q_{mBC} + \mathcal{H}_{,im}^{,22} P_{mBC} \\ &\quad + \mathcal{H}_{,mni}^{,112} Q_{mB} Q_{nC} + \mathcal{H}_{,nmi}^{,122} P_{mB} Q_{nC} + \mathcal{H}_{,mni}^{,122} Q_{mB} P_{nC} + \mathcal{H}_{,mni}^{,222} P_{mB} P_{nC}. \end{aligned} \tag{C.4}$$

Likewise,

$$\begin{aligned} \dot{P}_{iBC} &= -\mathcal{H}_{,im}^{,11} Q_{mBC} - \mathcal{H}_{,im}^{,12} P_{mBC} \\ &\quad + Q_{mB}\,[Q_{nC}\,\partial_n^1 + P_{nC}\,\partial_n^2](-\mathcal{H}_{,im}^{,11}) \\ &\quad + P_{mB}\,[Q_{nC}\,\partial_n^1 + P_{nC}\,\partial_n^2](-\mathcal{H}_{,im}^{,12}), \end{aligned}$$

so therefore,

$$\begin{aligned}\dot{P}_{iBC} &= -\mathcal{H}_{,im}^{,11}Q_{mBC} - \mathcal{H}_{,im}^{,12}P_{mBC} \\ &\quad -\mathcal{H}_{,imn}^{,111}Q_{mB}Q_{nC} - \mathcal{H}_{,inm}^{,112}P_{mB}Q_{nC} - \mathcal{H}_{,imn}^{,112}Q_{mB}P_{nC} - \mathcal{H}_{,imn}^{,122}P_{mB}P_{nC}. \end{aligned} \tag{C.5}$$

Using equations (C.4) and (C.5) we obtain,

$$\begin{aligned}P_{iA}\dot{Q}_{iBC} &= \mathcal{H}_{,mi}^{,12}P_{iA}Q_{mBC} + \mathcal{H}_{,im}^{,22}P_{iA}P_{mBC} \\ &\quad +\mathcal{H}_{,mni}^{,112}P_{iA}Q_{mB}Q_{nC} + \mathcal{H}_{,nmi}^{,122}P_{iA}P_{mB}Q_{nC} \\ &\quad +\mathcal{H}_{,mni}^{,122}P_{iA}Q_{mB}P_{nC} + \mathcal{H}_{,mni}^{,222}P_{iA}P_{mB}P_{nC}, \end{aligned} \tag{C.6}$$

$$\begin{aligned}Q_{iA}\dot{P}_{iBC} &= -\mathcal{H}_{,im}^{,11}Q_{iA}Q_{mBC} - \mathcal{H}_{,im}^{,12}Q_{iA}P_{mBC} \\ &\quad -\mathcal{H}_{,imn}^{,111}Q_{iA}Q_{mB}Q_{nC} - \mathcal{H}_{,inm}^{,112}Q_{iA}P_{mB}Q_{nC} \\ &\quad -\mathcal{H}_{imn}^{,112}Q_{iA}Q_{mB}P_{nC} - \mathcal{H}_{,imn}^{,122}Q_{iA}P_{mB}P_{nC}. \end{aligned} \tag{C.7}$$

C1 A special case

Assume that the quantities P_{iA} and P_{iAB} can be expressed in terms of the slowness components p_i as

$$P_{iA} = p_i E_A, \qquad P_{iAB} = p_i F_{AB}. \tag{C.8}$$

Applying equation (C.8) in equations (C.6)–(C.6) yields

$$\begin{aligned}P_{iA}\dot{Q}_{iBC} &= \mathcal{H}_{,mi}^{,12}p_i Q_{mBC}E_A + \mathcal{H}_{,im}^{,22}p_i p_m E_A F_{BC} \\ &\quad +\mathcal{H}_{,mni}^{,112}p_i Q_{mB}Q_{nC}E_A + \mathcal{H}_{,nmi}^{,122}p_i p_m Q_{nC}E_A E_B \\ &\quad +\mathcal{H}_{,mni}^{,122}p_i p_n Q_{mB}E_A E_C, \end{aligned} \tag{C.9}$$

$$\begin{aligned}Q_{iA}\dot{P}_{iBC} &= -\mathcal{H}_{,im}^{,11}Q_{iA}Q_{mBC} - \mathcal{H}_{,im}^{,12}p_m Q_{iA}F_{BC} \\ &\quad -\mathcal{H}_{,imn}^{,111}Q_{iA}Q_{mB}Q_{nC} - \mathcal{H}_{,inm}^{,112}p_m Q_{iA}Q_{nC}E_B \\ &\quad -\mathcal{H}_{,imn}^{,112}p_n Q_{iA}Q_{mB}E_C - \mathcal{H}_{,imn}^{,122}p_m p_n Q_{iA}E_B E_C. \end{aligned} \tag{C.10}$$

In equation (C.9) we have also applied the property (A.5) of the Hamiltonian, which eliminates the term including the derivative $\mathcal{H}_{,imn}^{,222}$.

Using relations (A.2)–(A.4) in equations (C.9)–(C.10) leads to

$$\begin{aligned}P_{iA}\dot{Q}_{iBC} &= -2\eta_m Q_{mBC}E_A + E_A F_{BC} \\ &\quad +2\mathcal{H}_{,mn}^{,11}Q_{mB}Q_{nC}E_A - 2\eta_n Q_{nC}E_A E_B - 2\eta_m Q_{mB}E_A E_C, \end{aligned} \tag{C.11}$$

$$\begin{aligned} Q_{iA}\dot{P}_{iBC} &= -\mathcal{H}_{,im}^{;11}Q_{iA}Q_{mBC} + 2\eta_i Q_{iA}F_{BC} \\ &\quad -\mathcal{H}_{,imn}^{;111}Q_{iA}Q_{mB}Q_{nC} - 2\mathcal{H}_{,in}^{;11}Q_{iA}Q_{nC}E_B \\ &\quad -2\mathcal{H}_{,im}^{;11}Q_{iA}Q_{mB}E_C + 2\eta_i Q_{iA}E_B E_C. \end{aligned} \tag{C.12}$$

C2 Plane wavefront

The next step is to apply in equations (C.11)–(C.12) specifically the conditions for a plane wavefront. This means to set

$$E_A = \eta_i \mathcal{E}_{iA}, \tag{C.13}$$

$$F_{AB} = (-U_{ij} + 3\eta_i\eta_j)\mathcal{E}_{iA}\mathcal{E}_{jB}, \tag{C.14}$$

$$Q_{iA} = \mathcal{E}_{iA}, \tag{C.15}$$

$$Q_{iAB} = 0. \tag{C.16}$$

This yields,

$$\begin{aligned} P_{iA}\dot{Q}_{iBC} &= (-U_{jk} + 3\eta_j\eta_k)\eta_i\mathcal{E}_{iA}\mathcal{E}_{jB}\mathcal{E}_{kC} \\ &\quad +2\mathcal{H}_{,mn}^{;11}\mathcal{E}_{mB}\mathcal{E}_{nC}\,\eta_i\mathcal{E}_{iA} - 2\eta_n\mathcal{E}_{nC}\eta_i\mathcal{E}_{iA}\eta_j\mathcal{E}_{jB} - 2\eta_m\mathcal{E}_{mB}\eta_i\mathcal{E}_{iA}\eta_k\mathcal{E}_{kC} \\ &= (\eta_i\,U_{jk} - \eta_i\eta_j\eta_k)\,\mathcal{E}_{iA}\mathcal{E}_{jB}\mathcal{E}_{kC} \end{aligned} \tag{C.17}$$

and

$$\begin{aligned} Q_{iA}\dot{P}_{iBC} &= 2\eta_i\mathcal{E}_{iA}\,(-U_{jk} + 3\eta_j\eta_k)\mathcal{E}_{jB}\mathcal{E}_{kC} \\ &\quad -\mathcal{H}_{,imn}^{;111}\mathcal{E}_{iA}\mathcal{E}_{mB}\mathcal{E}_{nC} - 2\mathcal{H}_{,in}^{;11}\mathcal{E}_{iA}\mathcal{E}_{nC}\,\eta_j\mathcal{E}_{jB} \\ &\quad -2\mathcal{H}_{,im}^{;11}\mathcal{E}_{iA}\mathcal{E}_{mB}\,\eta_k\mathcal{E}_{kC} + 2\eta_i\eta_j\eta_k\mathcal{E}_{iA}\mathcal{E}_{jB}\mathcal{E}_{kC} \\ &= (8\eta_i\eta_j\eta_k - 2\eta_i\,U_{jk} - 2\eta_j\,U_{ik} - 2\eta_k\,U_{ij} - U_{ijk})\,\mathcal{E}_{iA}\mathcal{E}_{jB}\mathcal{E}_{kC}. \end{aligned} \tag{C.18}$$

Taking the difference yields,

$$Q_{iA}\dot{P}_{iBC} - P_{iA}\dot{Q}_{iBC} = (9\eta_i\eta_j\eta_k - 3\eta_i\,U_{jk} - 2\eta_j\,U_{ik} - 2\eta_k\,U_{ij} - U_{ijk})\,\mathcal{E}_{iA}\mathcal{E}_{jB}\mathcal{E}_{kC}. \tag{C.19}$$

In addition, we have

$$\begin{aligned} P_{iAB}\dot{Q}_{iC} &= p_i F_{AB}(\mathcal{H}_{,mi}^{;12}Q_{mC} + \mathcal{H}_{,im}^{;22}P_{mC}) \\ &= (\mathcal{H}_{,mi}^{;12}p_i Q_{mC} + \mathcal{H}_{,im}^{;22}p_i p_m E_C)F_{AB} \\ &= (-2\eta_m Q_{mC} + E_C)F_{AB}. \end{aligned} \tag{C.20}$$

Inserting as above yields

$$P_{iAB}\dot{Q}_{iC} = (-3\eta_i\eta_j\eta_k + \eta_k\,U_{ij})\,\mathcal{E}_{iA}\mathcal{E}_{jB}\mathcal{E}_{kC}. \tag{C.21}$$

Finally, we apply the results (C.18), (C.19), and (C.21) in equation (C.1), which yields the constraint relation for a plane wavefront,

$$\begin{aligned} v_i P_{iABC} &= Q_{iA}\dot{P}_{iBC} - P_{iA}\dot{Q}_{iBC} - P_{iAB}\dot{Q}_{iC} - P_{iAC}\dot{Q}_{iB} \\ &= \left(15\eta_i\eta_j\eta_k - 3\eta_i U_{jk} - 3\eta_j U_{ik} - 3\eta_k U_{ij} - U_{ijk}\right)\mathcal{E}_{iA}\mathcal{E}_{jB}\mathcal{E}_{kC}. \end{aligned} \tag{C.22}$$

LIST OF TABLES

LIST OF FIGURES

Table 1. Main mathematical symbols used in the paper. For multicomponent quantities the dimensions are specified.

Quantity	Dimension	Description
(x_1, x_2, x_3)	3	Cartesian coordinate system
$\mathbf{x} = (x_i)$	3	Position vector of the Cartesian coordinate system
$\mathbf{p} = (p_i)$	3	Slowness vector (momentum vector) of the Cartesian coordinate system
$\mathbf{w} = (w_r)$ $= (x_i, p_j)$	6	Phase-space vector of the Cartesian coordinate system
Ω		Reference ray
$\mathcal{H}(\mathbf{w})$		Hamiltonian
$\hat{\mathcal{H}}$		Constant value of the Hamiltonian
$\mathcal{N}$		Degree of the Hamiltonian
τ		Traveltime along the ray Ω
τ_0		Traveltime at the initial point of the ray Ω
c		Phase velocity
$\mathbf{v} = (v_i)$	3	Ray-velocity (group-velocity) vector
$\boldsymbol{\eta} = (\eta_i)$	3	Derivative of slowness vector $\mathbf{p}$ with respect to traveltime τ
N_γ		Number of parameters specifying perturbation of the initial phase-space location. Possible values are 1 to 6.
(γ_a)	N_γ	Parameters specifying perturbation of the initial phase-space location
$\mathbf{X} = \{X_{ra}\}$	$6 \times N_\gamma$	Phase-space perturbation derivatives of first order
$\mathbf{S} = \{S_{rs}\}$	6×6	ODE coefficients related to first-order perturbation derivatives
$\mathbf{U} = \{U_{ij}\}$	3×3	Sub-set (sub-matrix) of the ODE coefficients $\{S_{rs}\}$
$\mathbf{V} = \{V_{ij}\}$	3×3	Sub-set (sub-matrix) of the ODE coefficients$\{S_{rs}\}$, the wave-propagation metric tensor
$\mathbf{W} = \{W_{ij}\}$	3×3	Sub-set (sub-matrix) of the ODE coefficients$\{S_{rs}\}$
$\delta\mathbf{w} = (\delta w_r)$	6	Perturbation of the phase space vector
$\delta\mathbf{w}_0 = (\delta w_r)_0$	6	Perturbation of the phase space vector at the initial point on Ω
$\boldsymbol{\Pi}(\tau, \tau_0)$ $= \{\Pi_{rs}(\tau, \tau_0)\}$	6×6	Ray propagator matrix
Π		Paraxial plane
$\boldsymbol{\mathcal{E}} = \{\mathcal{E}_{iM}\}$ $= [\mathbf{e}_1\ \mathbf{e}_2]$	3×2	Basis vectors in the plane Π
$\mathbf{H} = \{H_{ij}\}$ $= [\boldsymbol{\mathcal{E}}\ \mathbf{v}]$	3×3	Transformation matrix related to the plane Π
$\boldsymbol{\mathcal{F}} = \{\mathcal{F}_{iM}\}$	3×2	Sub-matrix of the 3×3 matrix $\mathbf{H}^{-T}$.
$\{\alpha_{ij}\}$	3×3	Projection operator with respect to the wave-propagation metric tensor

Table 1. – *continued*

Quantity	Dimension	Description
$\mathbf{M} = \{M_{ij}\}$	3×3	Second-order derivattives of traveltime with respect to Cartesian coordinates, on Ω
$\{M_{ijk}\}$	$3 \times 3 \times 3$	Third-order derivattives of traveltime with respect to Cartesian coordinates, on Ω
$\{M_{ijkl}\}$	$3 \times 3 \times 3 \times 3$	Fourth-order derivattives of traveltime with respect to Cartesian coordinates, on Ω
$\{Q_{ia}\}$, $\{P_{ia}\}$	$3 \times N_\gamma$	Phase-space perturbation derivatives of first order, in Q-P notation
$\mathbf{Q} = \{Q_{iA}\}$, $\mathbf{P} = \{P_{iA}\}$	3×2	Phase-space perturbation derivatives of first order, in Q-P notation, for the case $N_\gamma = 2$
$\widehat{\mathbf{Q}} = [\mathbf{Q}\ \mathbf{v}]$	3×3	Extension of matrix $\mathbf{Q}$ to size 3×3, the geometrical spreading matrix
$\widehat{\mathbf{P}} = [\mathbf{P}\ \boldsymbol{\eta}]$	3×3	Extension of matrix $\mathbf{P}$ to size 3×3
$\widehat{\mathbf{Q}}^\dagger = \{Q^\dagger_{ij}\} = \widehat{\mathbf{Q}}^{-1}$	3×3	Inverse geometrical spreading matrix
$\mathbf{Q}^\dagger = \{Q^\dagger_{Ij}\}$	2×3	Sub-matrix of the inverse geometrical spreading matrix
$\{X_{rab}\}$	$6 \times N_\gamma \times N_\gamma$	Phase-space perturbation derivatives of second order
$\{Q_{iab}\}$, $\{P_{iab}\}$	$3 \times N_\gamma \times N_\gamma$	Phase-space perturbation derivatives of second order, in Q-P notation
$\{S_{rst}\}$	$6 \times 6 \times 6$	Main ODE coefficients related to second-order perturbation derivatives
$\{R_{rst}\}$	$6 \times 6 \times 6$	Additional ODE coefficients related to second-order perturbation derivatives
$\{U_{ijk}\}$	$3 \times 3 \times 3$	Sub-set of the ODE coefficients $\{S_{rst}\}$
$\{V_{ijk}\}$	$3 \times 3 \times 3$	Sub-set of the ODE coefficients $\{S_{rst}\}$
$\{X_{rabc}\}$	$6 \times N_\gamma \times N_\gamma \times N_\gamma$	Phase-space perturbation derivatives of third order
$\{Q_{iabc}\}$, $\{P_{iabc}\}$	$3 \times N_\gamma \times N_\gamma \times N_\gamma$	Phase-space perturbation derivatives of third order, in Q-P notation
$\{S_{rstu}\}$	$6 \times 6 \times 6 \times 6$	Main ODE coefficients related to third-order perturbation derivatives
$\{R_{rstu}\}$	$6 \times 6 \times 6 \times 6$	Additional ODE coefficients related to third-order perturbation derivatives

Table 1. – *continued*

Quantity	Dimension	Description
$\mathbf{s} = (s_i)$	3	Source point
$\mathbf{r} = (r_i)$	3	Receiver point
$T(\mathbf{r}, \mathbf{s})$		Traveltime as a function of source-receiver coordinates
$\mathcal{L}(\mathbf{r}, \mathbf{s})$		Relative geometrical spreading as a function of source-receiver coordinates
$\{a_{ijkl}\}$	$3 \times 3 \times 3 \times 3$	Density-normalized elastic moduli
$\mathbf{\Gamma} = \{\Gamma_{ij}\}$	3×3	Christoffel matrix
G		Eigenvalue of the Christoffel matrix
P, Q, R		General invariants of the Christoffel matrix, for arbitrarily anisotropic media
P^{PSV}, R^{PSV}, G^{SH}		Particular invariants of the Christoffel matrix, for transversely isotropic media
G^{P}, G^{SV}		Particular invariants of the Christoffel matrix, for elliptically anisotropic media
$\mathbf{0}$	*	Zero multicomponent quantity. The dimensions follow from the context.
$\mathbf{I}$	3×3	Identity matrix
$\mathbf{J}$	6×6	Matrix for rearranging derivatives in Hamilton's equations

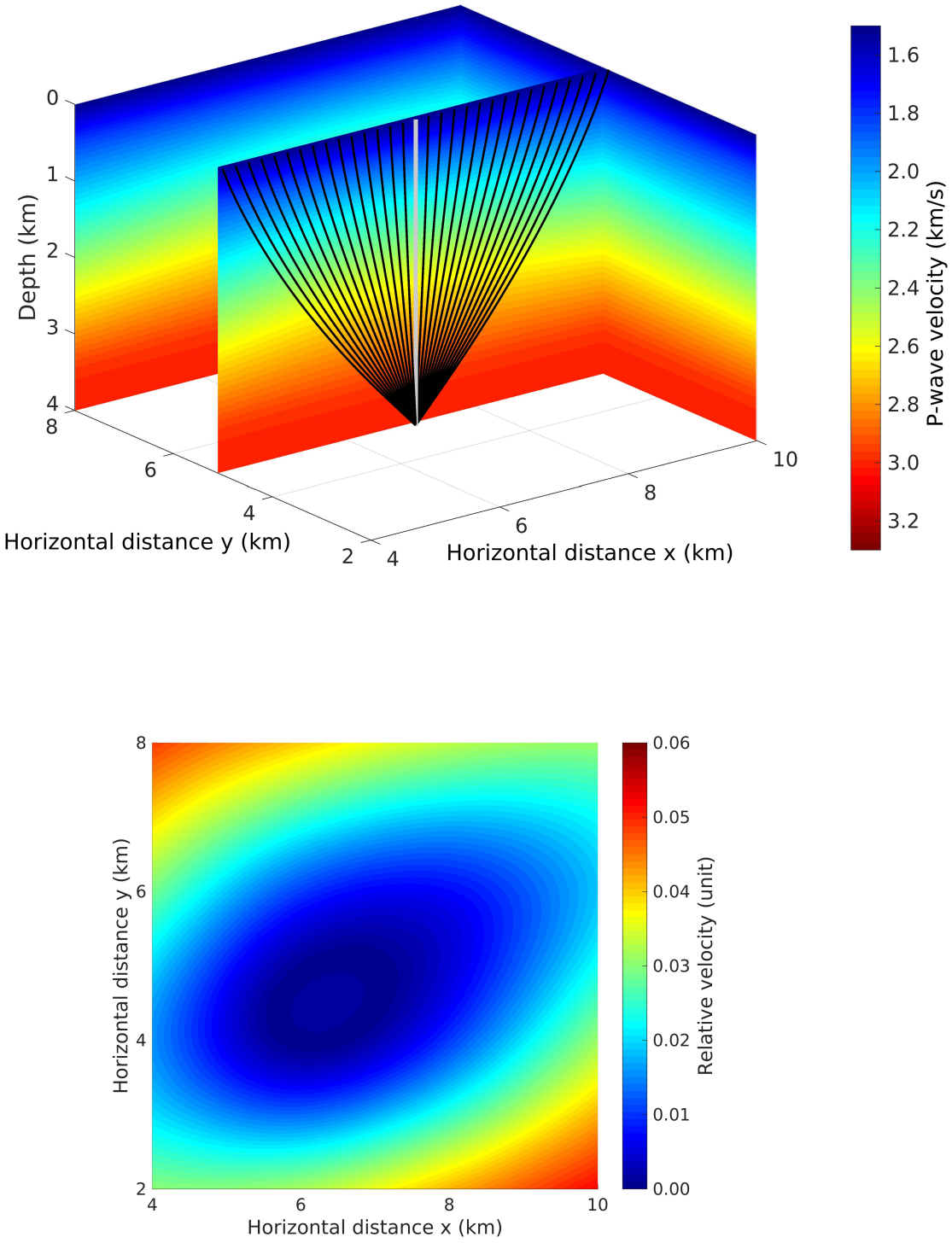

Figure 1. Model ISO and some of the rays used in numerical tests. (Top) The vertical P-wave velocity is indicated by color in vertical slices. Data for numerical comparisons is computed along rays (black) from a source point at depth 4 km. Coefficients for extrapolation of ray quantities are computed along a single reference ray (grey). (Bottom) Lateral differences in the vertical P-wave velocity, relative to the velocity on the reference ray, at depth 2 km.

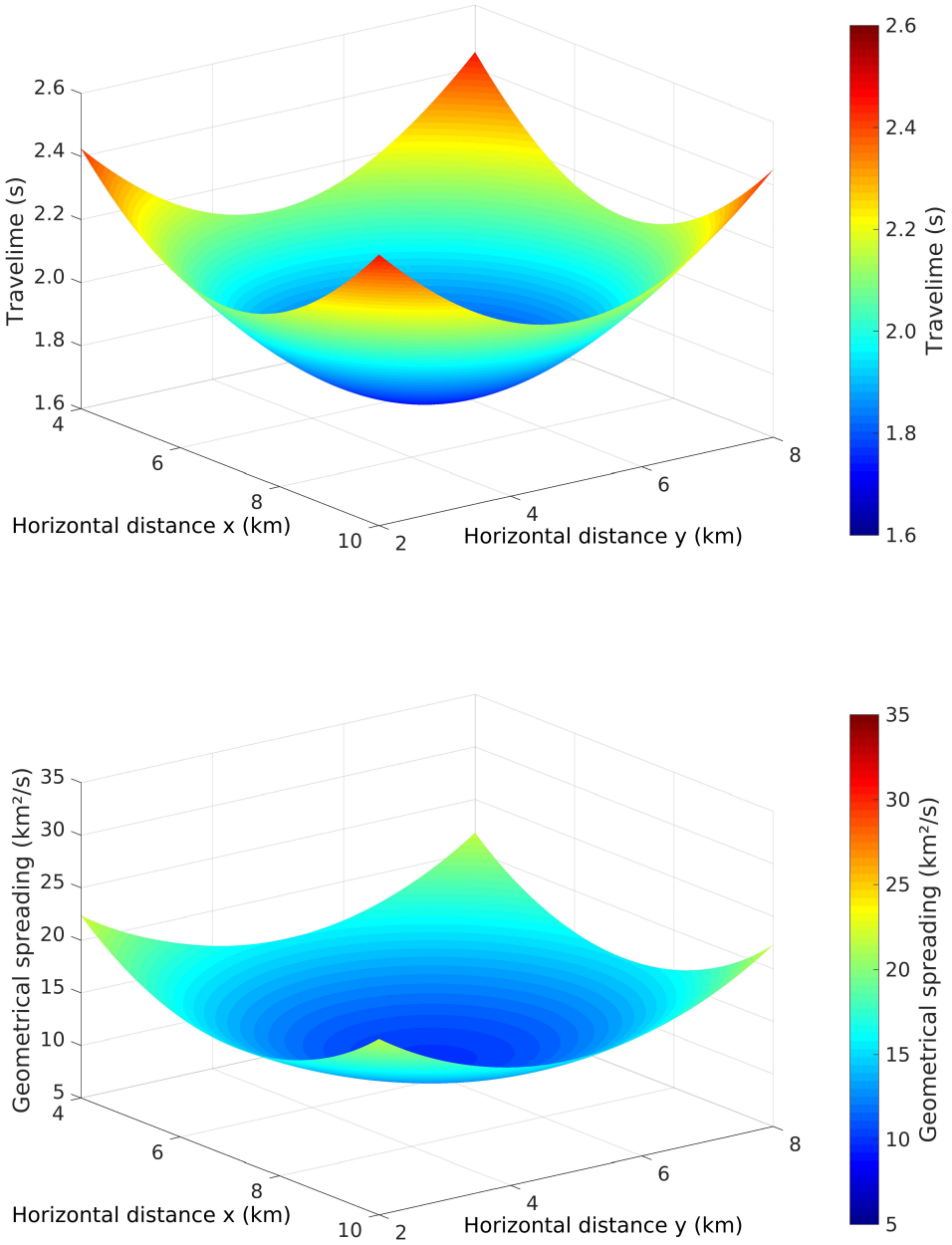

Figure 2. Model ISO: Ray-tracing simulated P-wave traveltime (top) and geometrical spreading (bottom) in the plane at depth 0 km for a source point at depth 4 km.

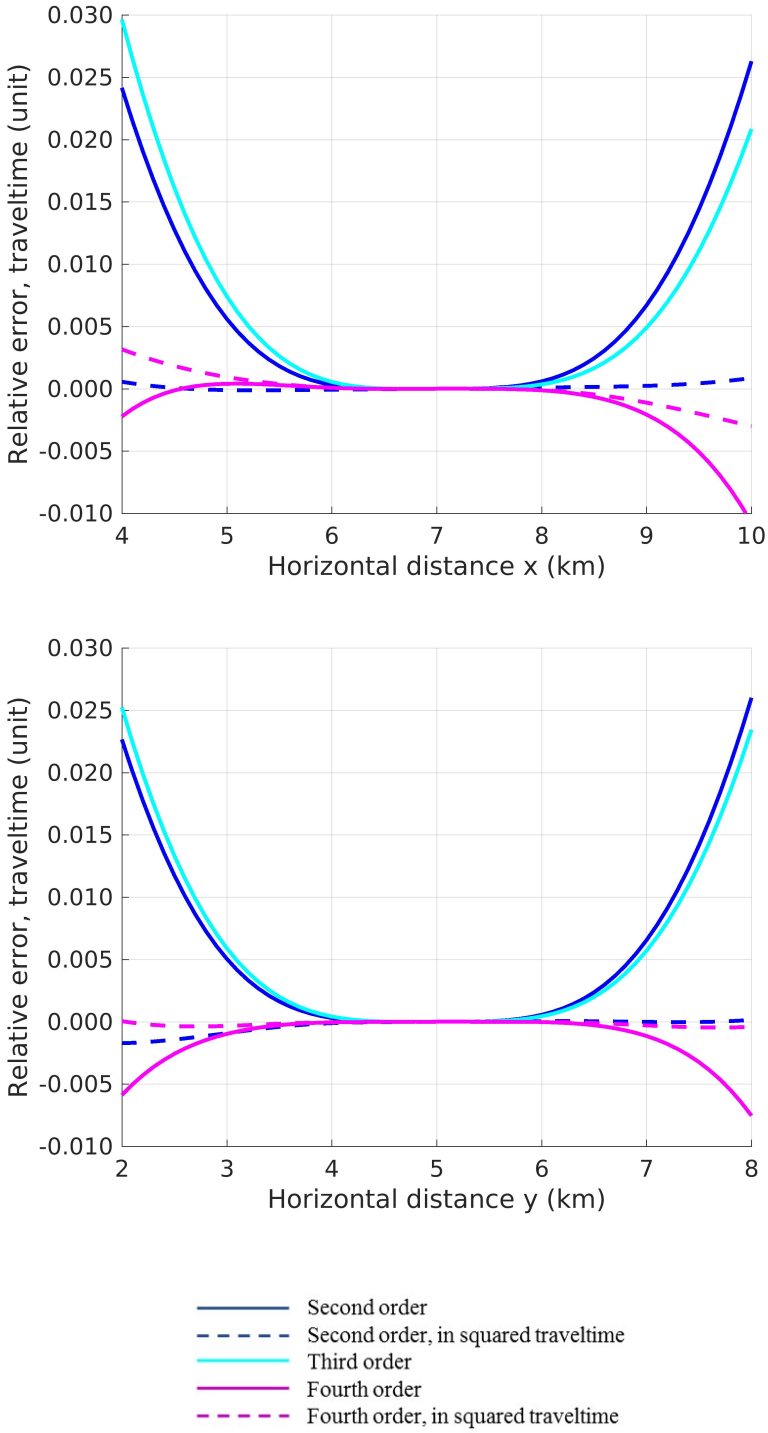

Figure 3. Model ISO: Relative error in traveltime for different extrapolation approaches along the lines y = 5 km (top) and x = 7 km (bottom).

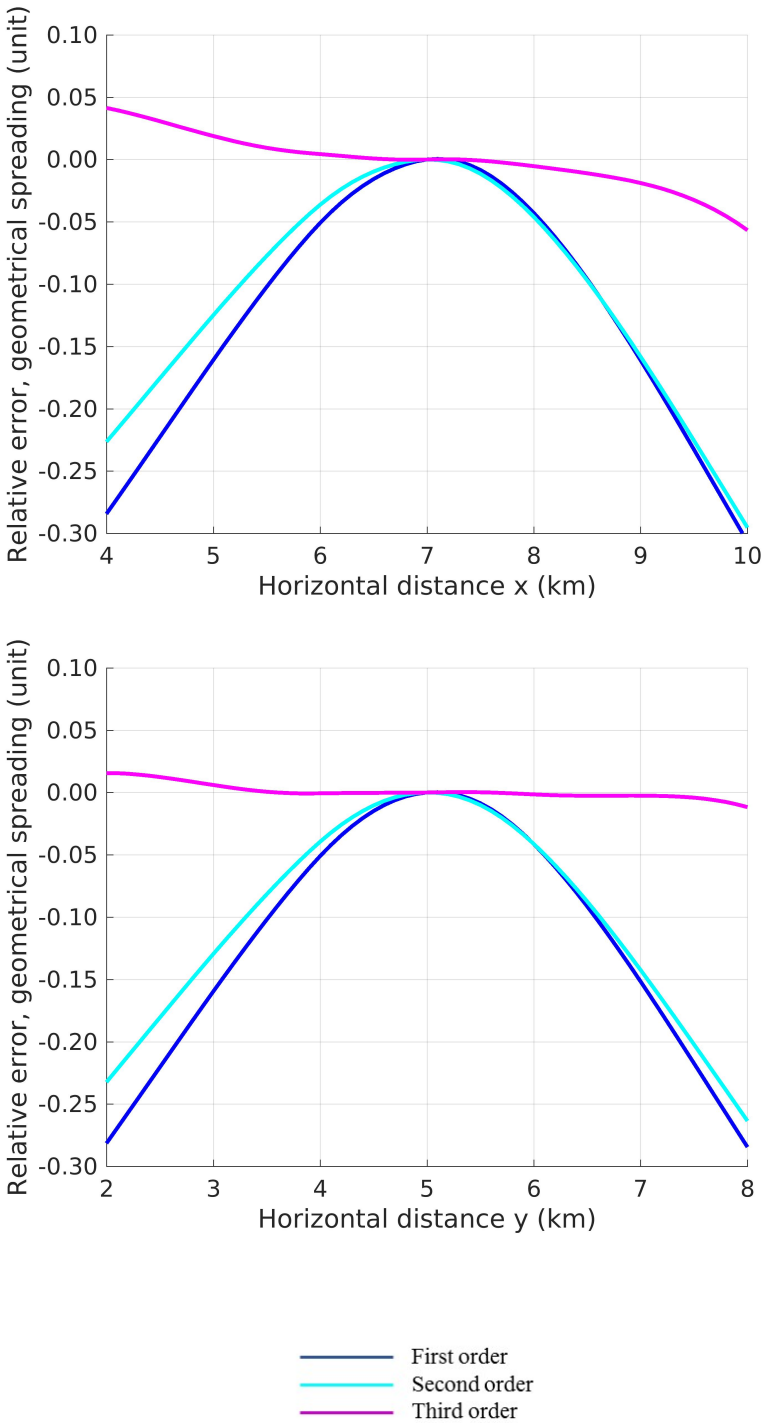

Figure 4. Model ISO: Relative error in geometrical spreading for different extrapolation approaches along the lines y = 5 km (top) and x = 7 km (bottom).

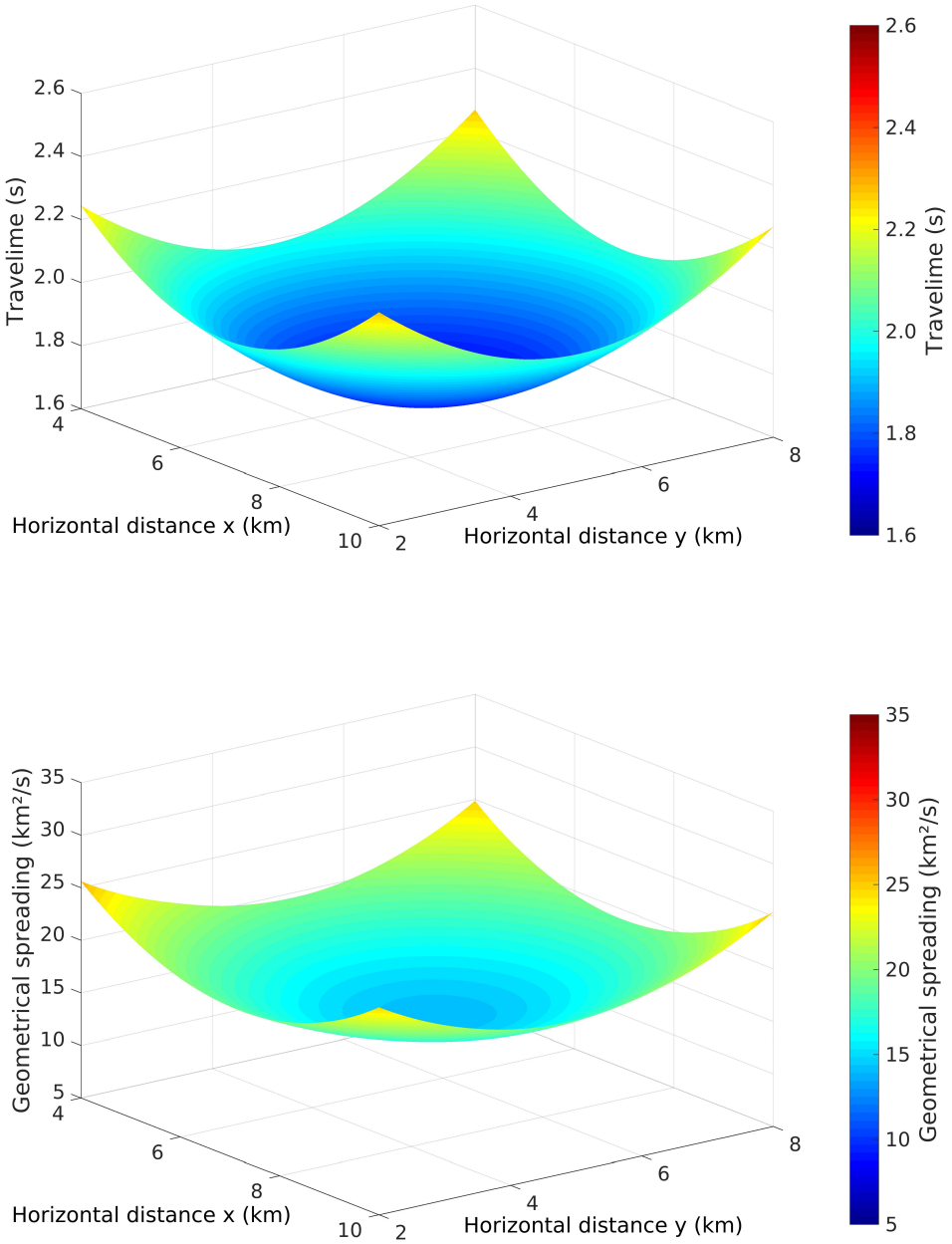

Figure 5. Model VEL: Ray-tracing simulated P-wave traveltime (top) and geometrical spreading (bottom) in the plane at depth 0 km for a source point at depth 4 km.

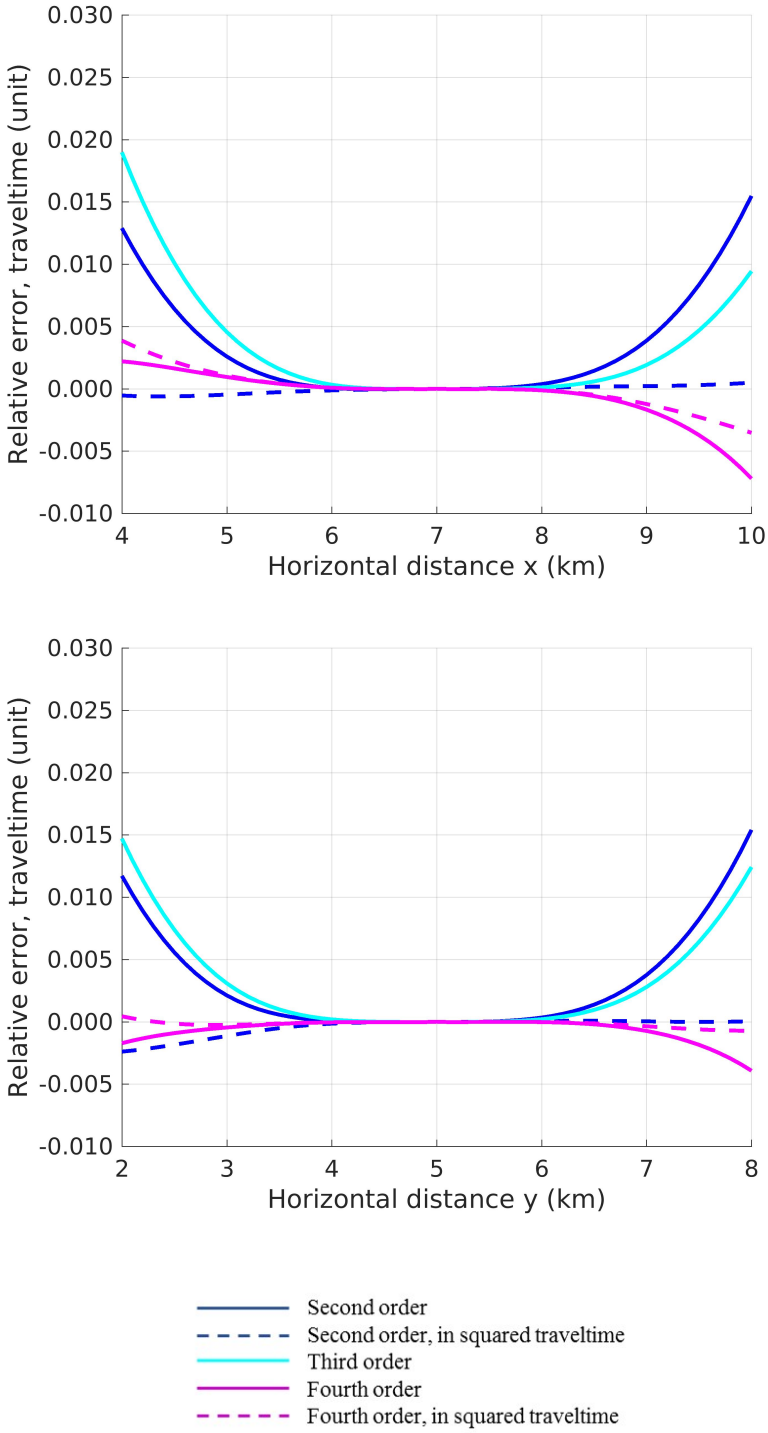

Figure 6. Model VEL: Relative error in traveltime for different extrapolation approaches along the lines y = 5 km (top) and x = 7 km (bottom).

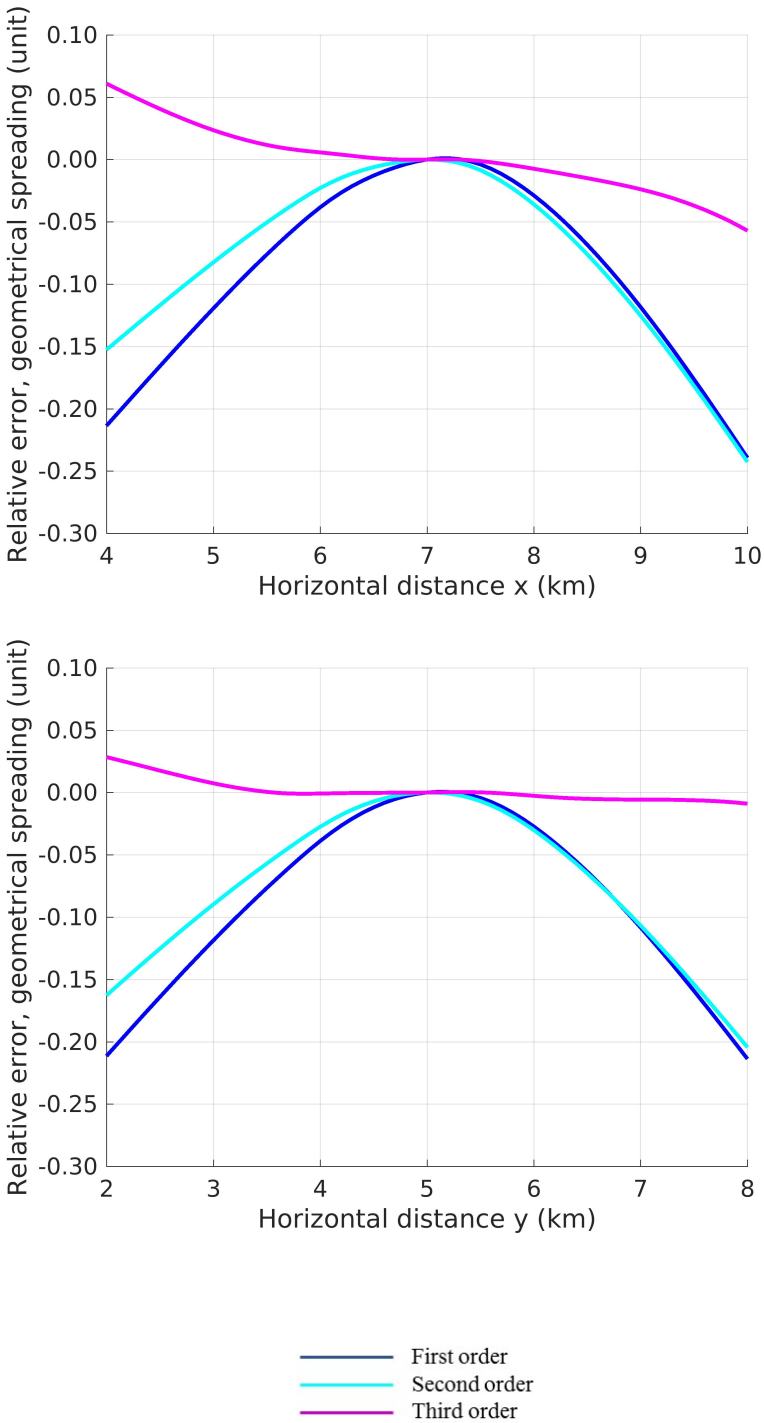

Figure 7. Model VEL: Relative error in geometrical spreading for different extrapolation approaches along the lines y = 5 km (top) and x = 7 km (bottom).

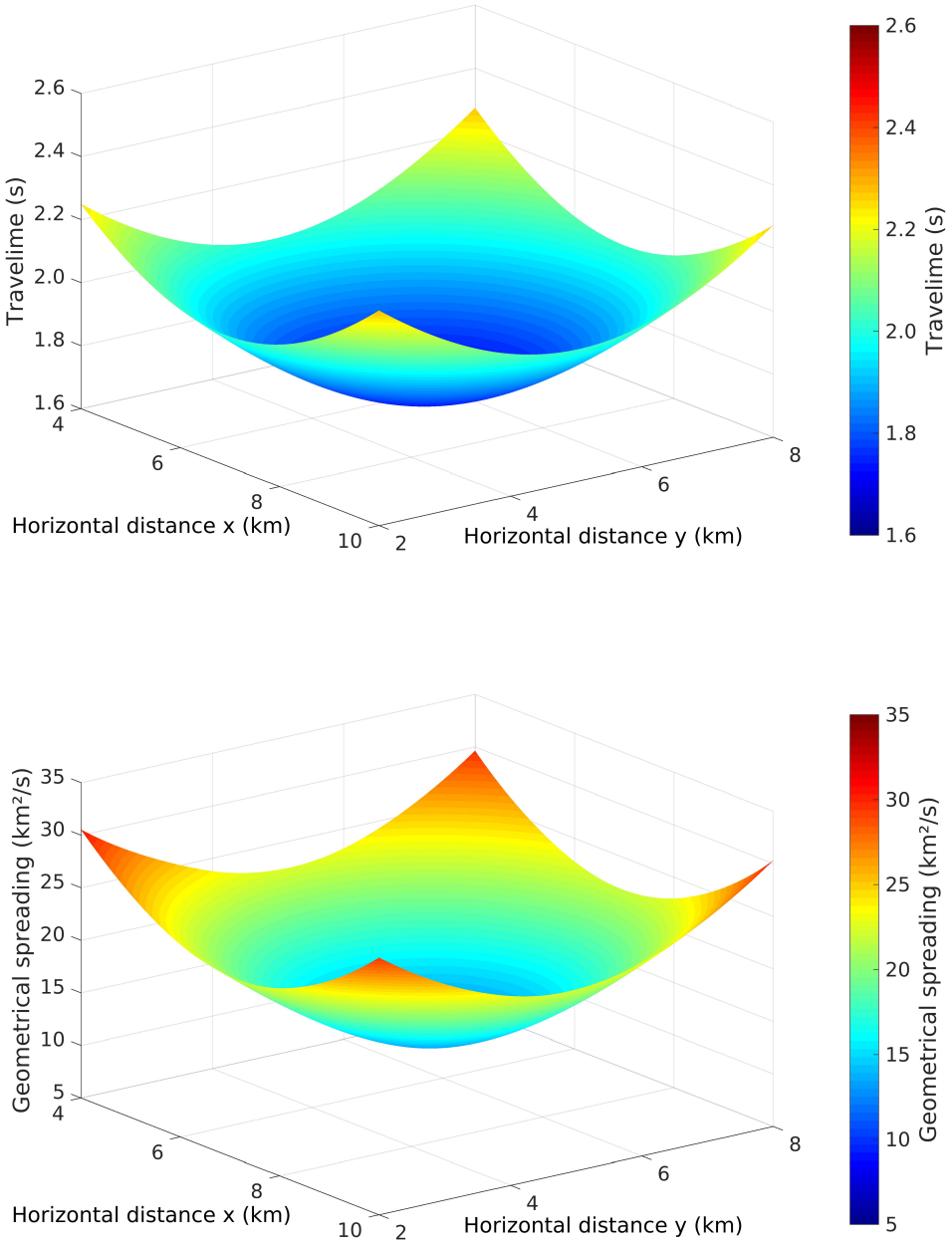

Figure 8. Model VTI: Ray-tracing simulated P-wave traveltime (top) and geometrical spreading (bottom) in the plane at depth 0 km for a source point at depth 4 km.

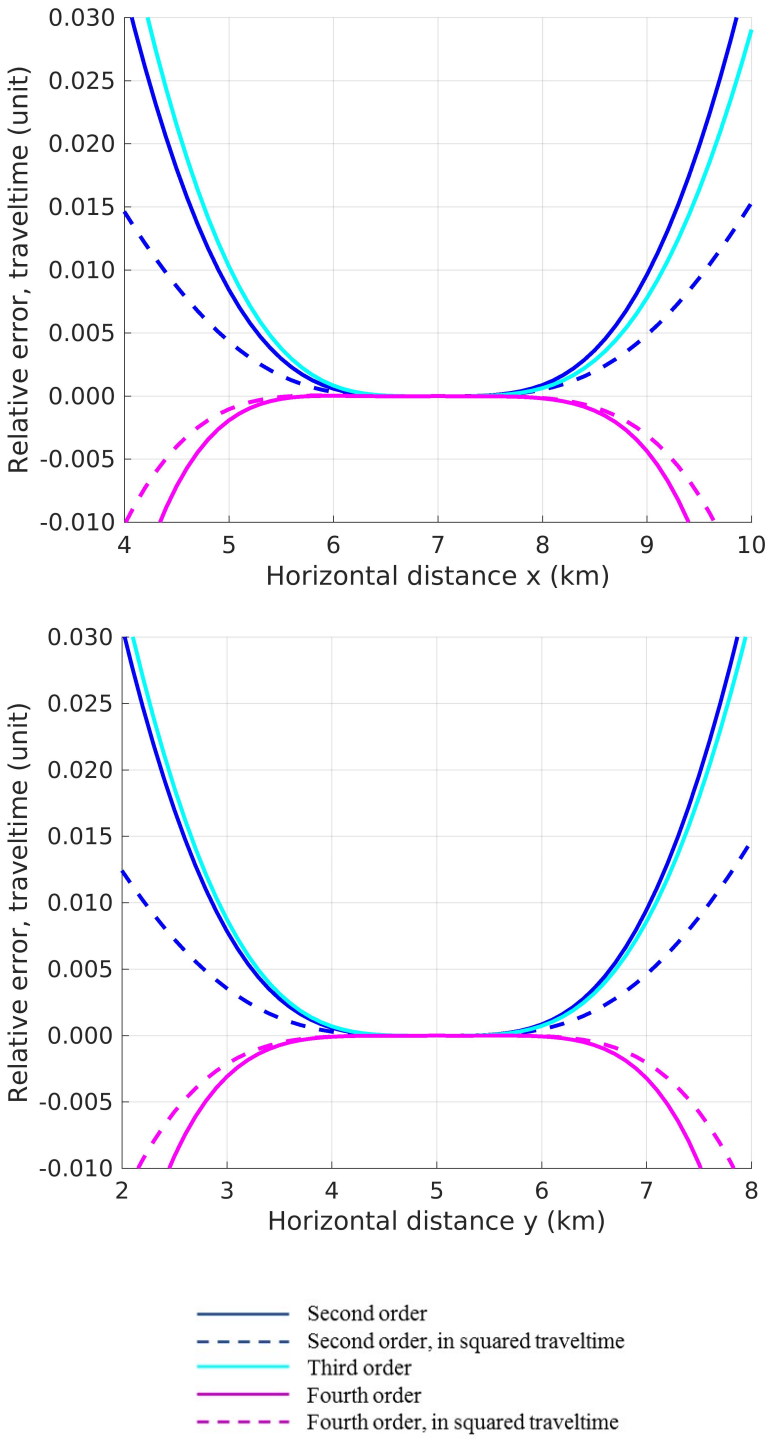

Figure 9. Model VTI: Relative error in traveltime for different extrapolation approaches along the lines y = 5 km (top) and x = 7 km (bottom).

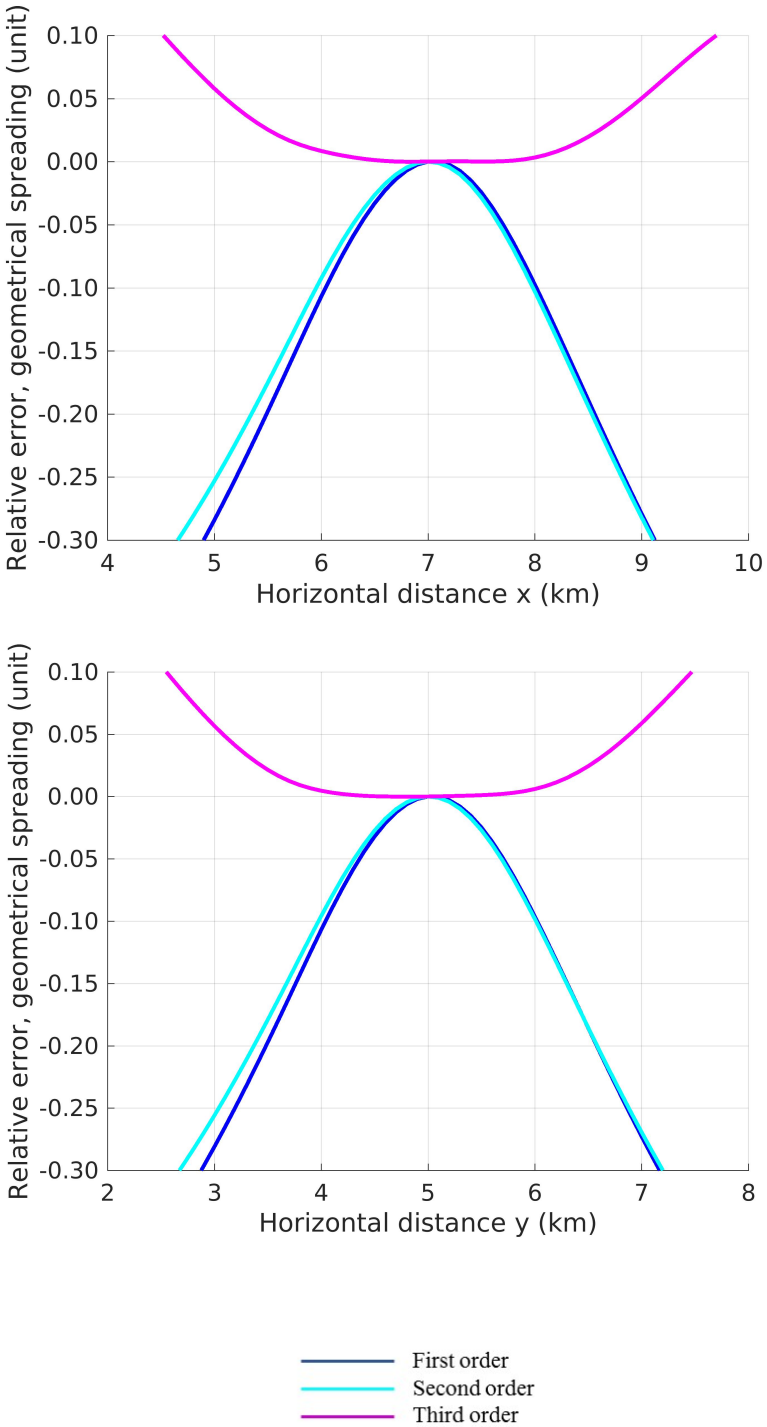

Figure 10. Model VTI: Relative error in geometrical spreading for different extrapolation approaches along the lines y = 5 km (top) and x = 7 km (bottom).